Enhanced Warming and Wetting of the Active Layer Caused by Rain and Snow, Svalbard

Bachelor Thesis by Saskia Marie Bacher

May 2019

Student Number 780372

Project Coordinator PD Dr. Julia Boike & Prof. Dr. Axel Bronstert

Statutory Declaration

I hereby declare that I have authored this thesis independently, that I have not used other than the declared resources and that I have explicitly marked all material, which has been quoted either literally or by content from the used sources. This work was not previously presented to another examination board and has not been published.

Date and Signature:

Abstract

The active layer situated between the permafrost and the ground surface has changed greatly over the last decades at a site in Ny-Ålesund, Svalbard. While permafrost is defined as ground (soil or rock) which has been below a temperature of 0 °C for at least two consecutive years, the active layer is thawing every summer and refreezing in autumn. Svalbard has the warmest permafrost compared to other Arctic sites at the same latitude.

In this study, meteorological data from 1998-2018 as well as soil temperature and active layer volumetric water content data were analysed. While the mean annual air temperature in Ny-Ålesund has increased over the past 20 years by about 1.46 °C (+/- 0.05 °C) per decade, the annual liquid precipitation sum increased by 76 mm (+/- 44 mm) per decade. Furthermore, the timespan when the ground is covered by snow has shortened. The active layer has doubled in thickness from around 90 cm in 1998 to more than 150 cm in 2018. The freezing period starts later compared to 20 years ago, leading to a shortening of the period when the soil is frozen of 31 days (+/- 17 days) per decade. During the 20 years of observation, the active layer always completely refroze in winter, but the liquid volumetric water content remained partly above 10 %.

The analysis of the active layer temperature and the liquid volumetric water content revealed a general warming and wetting trend within the 20 years of observation. In the active layer soil warming is normally reduced as energy is used for melting of ground ice. This process usually increases the liquid volumetric water content. Still, over the 20 year period the soil temperature increased by 0.9 °C to 1.6 °C (+/- 0.6 °C) per decade as a range for all measured depths (4 cm – 133 cm). The mean annual LVWC in the active layer at 10 cm to 94 cm depth increased as a range for the depths between 0.6 % and 3.2 % (+/- 1.2 %) per decade. The main correlating parameters to the changes in soil temperature and liquid volumetric water content of the soil for each month were assessed using a correlation matrix. The main correlation factor seems to be in winter and spring the lengthening of the thawing period, in summer the earlier vanishing snow cover and in autumn the delayed start of the freeze-back period. However, these parameters are in turn influenced by air temperature and precipitation changes. Surface

volumetric water content declined slightly over the 20 years by about 1.7% (+/- 0.6 %) per decade, probably due to stronger evapotranspiration or due to the deepening of the active layer. If the trend of the past 20 years continued, permafrost degradation on Svalbard could be increasing over the next years causing landscape changes, landslides and stronger erosion, posing a potential-risk to infrastructure.

Kurzfassung (dt.)

Die Auftauschicht, zwischen Bodenoberfläche und Permafrost gelagert, hat sich stark über die letzten 20 Jahre an einer Messstelle in der Nähe von Ny-Ålesund, Spitzbergen verändert. Während Permafrost als Untergrund definiert ist (Boden oder Gestein), der sich fortlaufend über zwei Jahre unter einer Temperatur von 0°C befunden hat, taut die Auftauschicht jeden Sommer auf und gefriert im Herbst wieder. Spitzbergen hat den wärmsten Permafrost im Vergleich zu anderen arktischen Standorten auf dem gleichen Breitengrad.

Für die vorliegende Studie wurde eine statistische Analyse von meteorologischen Daten sowie Bodentemperatur- und Bodenfeuchtedaten (1998-2018) durchgeführt. Das Jahresmittel der Lufttemperatur hat sich innerhalb der 20 Jahre um 1.46 °C (+/- 0.05 °C) pro Dekade erhöht, während sich die jährliche Niederschlagssumme über den Zeitraum um 76 mm (+/- 44 mm) pro Dekade gesteigert hat. Des Weiteren hat sich der Zeitraum verkürzt, indem der Boden von Schnee bedeckt ist. Die Auftauschicht betrug im Jahr 1998 noch um die 90 cm und hat sich bis 2018 auf über 150 cm verdoppelt. Der Zeitraum, indem der Boden im Winter gefroren ist hat sich um 31 Tage (+/- 17 Tage) pro Dekade verkürzt. Während der 20 Jahre ist die Auftauschicht im Winter immer zurückgefroren, jedoch blieb die Bodenfeuchte teilweise über 10 %.

Die statistische Auswertung der Bodentemperatur und- feuchte der Auftauschicht ergab eine generelle Erwärmung und Befeuchtung des Bodens. In der Auftauschicht wird die Bodenerwärmung normalerweise reduziert, indem die Energie für das Schmelzen des Bodeneises genutzt wird. Die Bodenfeuchte steigt dabei. Das Ergebnis der Studie zeigt jedoch trotzdem eine Erwärmung des Bodens mit einer Spanne von 0.9 °C bis 1.6 °C (+/- 0.6 °C) pro Dekade für die Schichten 4 cm bis 133 cm. Die Bodenfeuchte in der Auftauschicht im Bereich 10 cm bis 94 cm ist mit einer Spanne von 0.6 % bis 3.2 % (+/- 1.2 %) pro Dekade gestiegen. Korrelierende Parameter für den Anstieg der Bodentemperatur und -feuchte in jedem Monat wurden mit Hilfe einer Korrelationsmatrix gefunden. Der primäre korrelierende Parameter im Winter und Frühling ist die Verlängerung Zeitspanne indem der Boden getaut ist, im Sommer der Zeitpunkt, wenn der Schnee vollständig geschmolzen ist und im Herbst der Zeitpunkt,

wenn das Zurückfrieren des Bodens beginnt. Alle Parameter sind jedoch abhängig von der Lufttemperatur und dem Niederschlag. Die Feuchtigkeit im Oberboden (4 cm Tiefe) hat sich um 1.7 % (+/- 0.6 %) pro Dekade verringert, wahrscheinlich durch höhere Evapotranspiration oder durch die Vertiefung der Auftauschicht. Wenn der Trend der letzten 20 Jahre anhält, könnte es zu starker Permafrostdegradierung in den nächsten Jahren auf Spitzbergen kommen, wodurch Landschaftsveränderungen, Hangrutsche und stärkere Erosion ausgelöst werden könnten, welche wiederum ein Risiko für die Infrastruktur darstellen.

Contents

List of Figures

List of Tables

Abbreviations

GTN-P Global Terrestrial Network for Permafrost

IPY International Polar Year

Ts Soil temperature

LVWC Liquid volumetric water content

ZAA Zero Annual Amplitude

1. Introduction

Permafrost occurs under 9 % - 12 % of the global land surface (Vaughan et al., 2013), but can also be found submarine. Permafrost is defined as ground (soil or rock), which has remained consecutively below a temperature of 0 °C for at least two years (Harris et al., 1988). If the soil contains liquid or frozen water, the term frozen permafrost can be used, but water is no prerequisite. Large regions in the Arctic are underlain by permafrost, affecting ecosystems, hydrology and other processes.

Permafrost conditions are altered by air temperatures, but the influence can be subdued by the surface conditions (i.e. snow, plants) (Christiansen et al., 2019). Zhang et al. (1998) also underlined that air temperature has the greatest influence on the soil temperature, while the seasonal snow cover and volumetric water content are secondary factors.

Romanovsky et al. (2010) stated a general rise in air temperature in the Northern region since the 1980s and with it an overall rise in permafrost temperatures. For Svalbard, an archipelago north of Norway, Førland et al. (2011) indicated an increase in average winter air temperature by 3.4 °C in 1991 - 2010, compared to the period of 1961 - 1990. Svalbard has the warmest permafrost for its latitude with only a few degrees below the freezing point (Romanovsky et al., 2010). For a mountainous permafrost site on Svalbard Isaksen et al. (2007) calculated a warming trend of the permafrost table of 0.6 - 0.7 °C per decade since 1999.

The Arctic precipitation increased by approximately 8 % over the past century especially as rain in winter and autumn (ACIA, 2004). Førland et al. (2011) stated a general rise in total precipitation in all monitored regions of the Arctic (1961 - 2011) with an increase of 3 – 4 % per decade in Ny-Ålesund, the northernmost settlement on Svalbard.

Ground temperatures of cold permafrost and of permafrost in bedrock show a greater response to warming air temperatures than ground temperatures of warm permafrost where latent heat effects occur (Romanovsky et al., 2010). In permafrost close to the 0 °C boundary, ground ice is melting. During this process, energy is converted into latent heat while the ground temperature stabilizes around 0 °C. Hence, the temperature of the soil is often not or less enhanced. Ice- rich permafrost has also a higher thermal stability than ice-poor permafrost due to the same mechanism. Nicolsky and Romanovsky (2018) also underlined the importance of the liquid water content in the soil as it can decrease the thawing rate of the permafrost soil.

Liquid water content and ground thaw generally feedback on each other (Guan et al., 2010a). The liquid water content has an influence on the thermal conductivity of the soil and the available heat energy for ground thaw, while the deeper the ground thaw is the more water can be stored in the ground (Guan et al., 2010b). The thaw depth has increased at some sites in the Arctic, while others show no increase (Romanovsky et al., 2011).

As a response to changing ground conditions, permafrost landscapes have been changing enormously over the last decade. Once the soil temperature rises above 0 °C and the ice in the soil starts to melt, thermokarst features, slumps, soil subsidence, coastal erosion or other landscape changes can occur (Kokelj and Jorgenson, 2013).

In the permafrost soil, large quantities of organic carbon are stored as the degradation of the plant material is restricted in cold areas. Microorganisms are restricted by the climate and soil conditions; hence the organic material can accumulate over years. With the warming and wetting of the soil, the microorganisms' activity increases and potentially mobilizes increased amounts of organic carbon. The Arctic has an incredible importance for the global carbon cycle and is counted as one of the tipping elements in the global climate system (Schuur et al., 2015; Lenton et al., 2008).

Climate models predict that Arctic air temperatures will rise further than already observed and climate warming derived from global circulation models (GCMs) is greater in the Arctic than anywhere else (ACIA 2004, Zhang et al., 1998). This would cause a change in multiple climate and soil variables such as air temperature, radiation, snow depth, precipitation and soil temperature, but the outcome at a local scale is uncertain (ACIA, 2004).

Local observations are crucial for observing changes and predicting the future response of permafrost to climate change. Permafrost boreholes have been installed across the Arctic often in combination with meteorological stations measuring basic climate variables such as air temperature, liquid precipitation and snow depth. The data is uploaded to databases such as "The Global Terrestrial Network for Permafrost" (GTN-P), “Nordicana D“ or “Pangaea”. Climatic changes can also be quantified by remote sensing (Westermann et al., 2011).

1.1 Objectives of this study

The aim of the study was to give an overview on changes in climate and soil variables that happened over the past 20 years at a research site on Svalbard. While air temperature change in the Arctic and Svalbard has been studied extensively, very few studies focused on changing liquid precipitation and liquid volumetric water content (LVWC), which are the main focus of the study here.

The working hypothesis was that the active layer at a site on Svalbard has warmed and got wetter over the past 20 years. The research questions were as follows:

- Has the onset and duration of the active layer freeze back changed? Does the active layer freeze back in winter completely?
- Has the LVWC of the active layer changed over the past 20 years and if yes, what might be the cause of observed changes?
- Can changes in the seasonal rain and snow patterns be observed and do those changes have a feedback on the soil conditions?

An investigation in long-term data from a site on Svalbard has been conducted. First, an introduction to the study site will be given, followed by a short description of the theoretical background (Chapter 2). Thereafter, the methodological approach will be shown (Chapter 3). Basic climate parameters from the past 20 years will be presented at the beginning of Chapter 4. The results from the analysis of the air temperature, the liquid precipitation, the snow depth, the active layer, the freezing period, the soil temperature and the LVWC will be presented (Chapter 4). In the end, the results will be discussed (Chapter 5) and summarized (Chapter 6).

1.2 Study site

Svalbard is an island group north of Norway situated between the Greenland Sea and the Barents Sea. Up to 60 % of the island group is covered by glaciers (Humlum et al., 2003). The remaining ice-free ground generally consists of continuous permafrost (Humlum et al., 2003; Liestøl, 1977). The permafrost thickness is estimated to be below 100 m near the coast and up to 400 – 500 m in the mountains (Humlum et al., 2003; Liestøl, 1977). In the IPY, the international polar year during 2007 – 2009, the permafrost temperatures in Svalbard varied locally at the depth of zero annual amplitude (if not measured deepest sensor in at least 4 m depth taken) depth between -2.3 °C and -5.6 °C (Christiansen et al., 2010).

The study site Bayelva, where all data is drawn from, is situated on a mineral hummock field 3 km west of Ny-Ålesund in the north-western part of Svalbard (Roth et al., 2001) (Figure 1). Bayelva is the name of the catchment area, which was studied intensely over the last years regarding sedimentation processes (Hodson et al., 2002), local climate and soil conditions (Boike et al., 2018; Roth et al., 2001) and vegetation (Cannone et al., 2004; Ohtsuka et al., 2006). The Bayelva river is fed by the Brøggerbreen glacier and creates a flat channel on its way to into Kongsfjorden, the fjord that is connected to the open ocean. The meteorological and soil station Bayelva (78°551'N, 11°571'E) is situated next to the river channel on the Leiherhaugen Hill at 30 m above sea level (Roth et al., 2001; Boike et al., 2018). The lowland area was deglaciated 11000 - 13000 years ago and is characterized by periglacial features at present (Cannone et al., 2004). The area in front of the glacier is dominated by tundra vegetation (Westermann et al, 2011) with bryophytes and vascular plants, but the composition of the species is strongly dependent on local conditions (Cannone et al., 2004; Ohtsuka et al., 2006). The Leiherhaugen Hill itself is showing non- sorted circles (Boike et al., 2018). Snow covers the soil for up to 9 months each year (Boike et al., 2018), but Førland and Hanssen- Bauer (2000) note that snow and rain can occur during all months of the year.

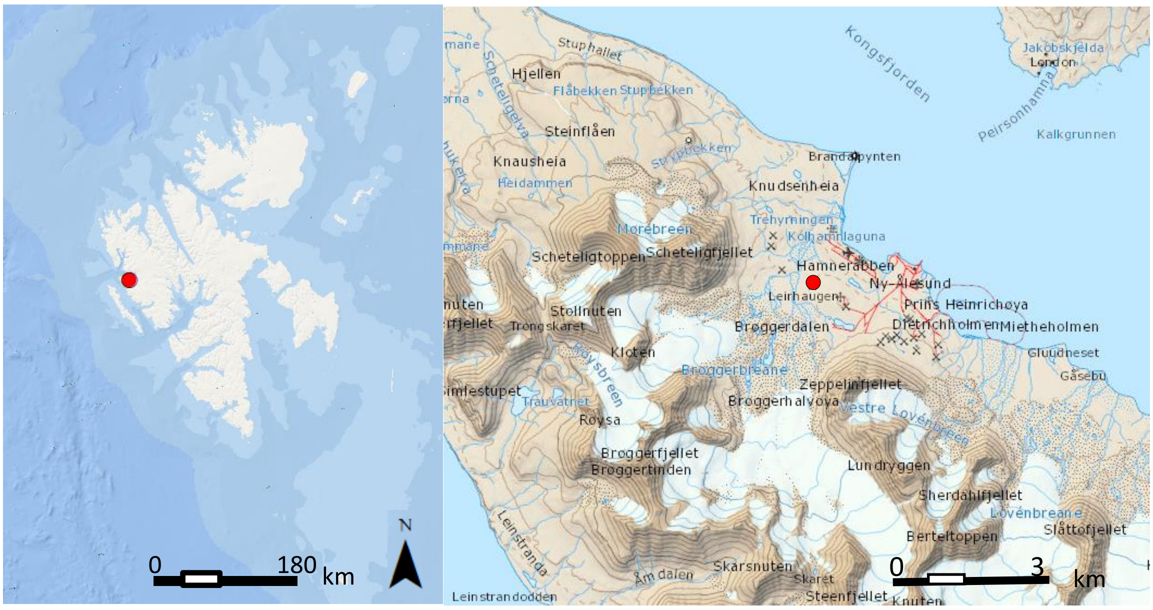

Figure 1: Location of the study site. Left: Archipelago Svalbard with Ny-Ålesund (red point) (ESRI, Arc GIS Basemap); Right: Topographic Map of the study area Ny-Ålesund with the Leiherhaugen Hill (red point) (TopoSvalbard: https://toposvalbard.npolar.no/).

According to Boike et al. (2018), the mean permafrost temperature at the site is -2.8 °C and the zero annual amplitude (ZAA) lies in 5.5 m depth (2009-2017). In 2016, the active layer above the permafrost reached 2 m depth according to Ebenhoch (2018).

1.3 Bayelva station

At Bayelva, meteorological data obtained by climate sensors can be distinguished from soil data drawn from soil stations. The meteorological and soil stations are situated directly on top of the Leiherhaugen Hill and are surrounded by a fence to protect the instruments from reindeer (see Figure 2). A 9 m deep borehole and an eddy covariance station are located nearby the fence (Boike et al., 2018).

The data from the station is of great importance as the data density of the region is low (Boike et al., 2018). The Norwegian Sverdrup Station started with the meteorological monitoring in 1969 (Boike et al., 2018). It collects basic meteorological data at the AWIPEV research station in Ny-Ålesund (http://awipev.eu/). The station Bayelva was established nearby in 1998 by the Alfred Wegener Institute (Boike et al., 2018). Hence a data series as long as 20 years is available (Boike et al., 2018).

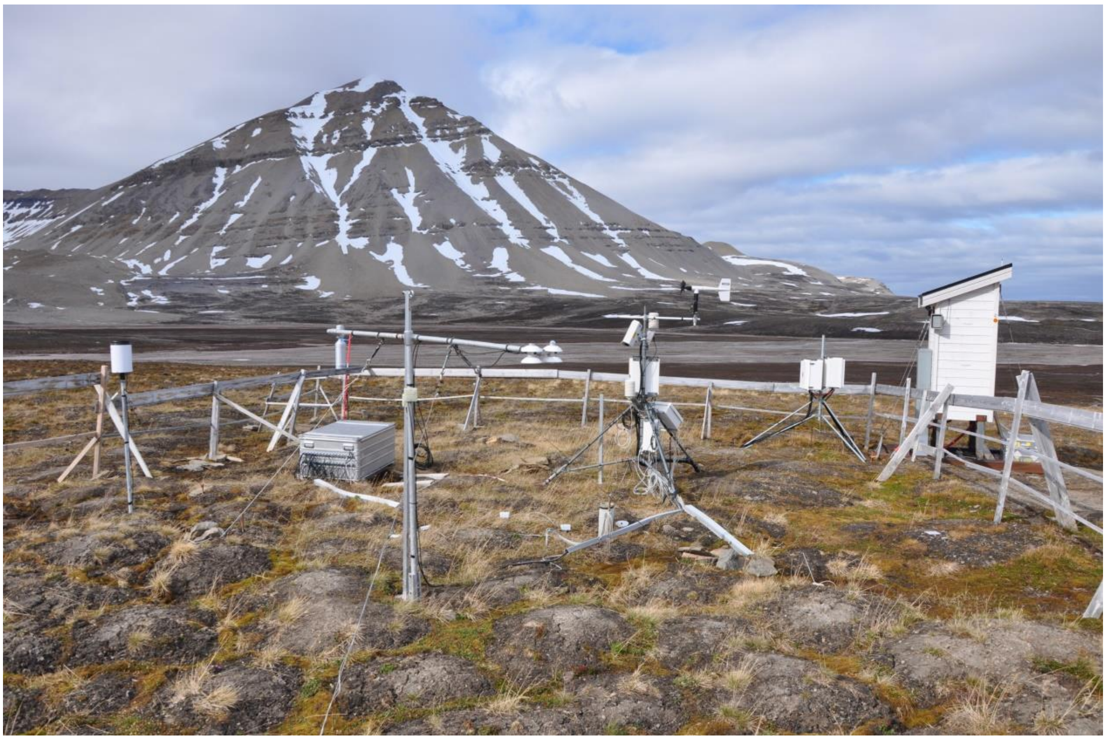

Figure 2: Bayelva meteorological station close to Ny-Ålesund during summer 2017 (Picture: Niko Bornemann)

1.3.1 The meteorological station

The meteorological station is measuring air temperature and humidity in different heights above the ground, incoming and outgoing long- and shortwave radiation (since 2009), liquid precipitation (tipping bucket gauge) and snow depth (using snow depth sensors and cameras). Air temperature and snow depth records, which are used in this study, go back to 1998 and 1999. An initial sensor measuring the air temperature was replaced in 2009. A second snow depth sensor (sonic ranging sensor SR50) was installed in 2006, a third in 2013. In this study the data from the first snow sensor was taken from 1999-2013 and from the third from 2013-2018.

1.3.2 The soil station

Several soil profiles were equipped around the meteorological station (Figure 3). The LVWC is measured next to soil temperature sensors in different depths. Data from different profiles but similar depths were used in this study as none of the data series spans over the whole period of 20 years. The soil profiles have a maximum depth of 1.4 m. A borehole of 9 m depth was established in 2009 but only with temperature sensors.

Figure 3: Topview on Bayelva soil temperature and liquid volumetric water content measurement field. Left: Data from profile (a) and (c) is used in this study. Right: Profile (c) from the left hand side here as drilled profile in summer 2009 with temperature and time domain reflectometry (TDR) sensors. Pictured from Boike et al. 2018.

Two soil profiles (a, c in Figure 3) were combined for the analysis of the ground thermal regime (for information about the combined sensors see the methodology part, section 3). Therefore, measurements for soil temperature from 4 cm to 133 cm and for LVWC from 4 cm to 94 cm are available over a time span of 20 years. The LVWC is derived from TDR (time domain reflectometry) measurements.

2. Theoretical background

2.1 Ground thermal regime of permafrost

The thermal state of permafrost can be described with the help of a trumpet curve (Figure 4). The absolute highest and lowest temperatures of each depth are plotted against depth. The timespan of the dataset is not predefined, but often a timespan of one year is used to get the maximum and minimum temperatures from the year. The annual temperature amplitude decreases with depth down to the point where it becomes negligible (<0.1 °C), referred to as the depth of zero annual amplitude (ZAA). Below the ZAA, there is no crucial difference between maximum and minimum, which means the temperature is not changing during the course of one year. The temperature gradient below the ZAA reflects the geothermal gradient (French 2007, Strand 2016). The so-called permafrost table can be found at the depth where the maximum curve intersects with the 0 °C-isoline. The area above the permafrost table, but below the surface is called the **active layer**.

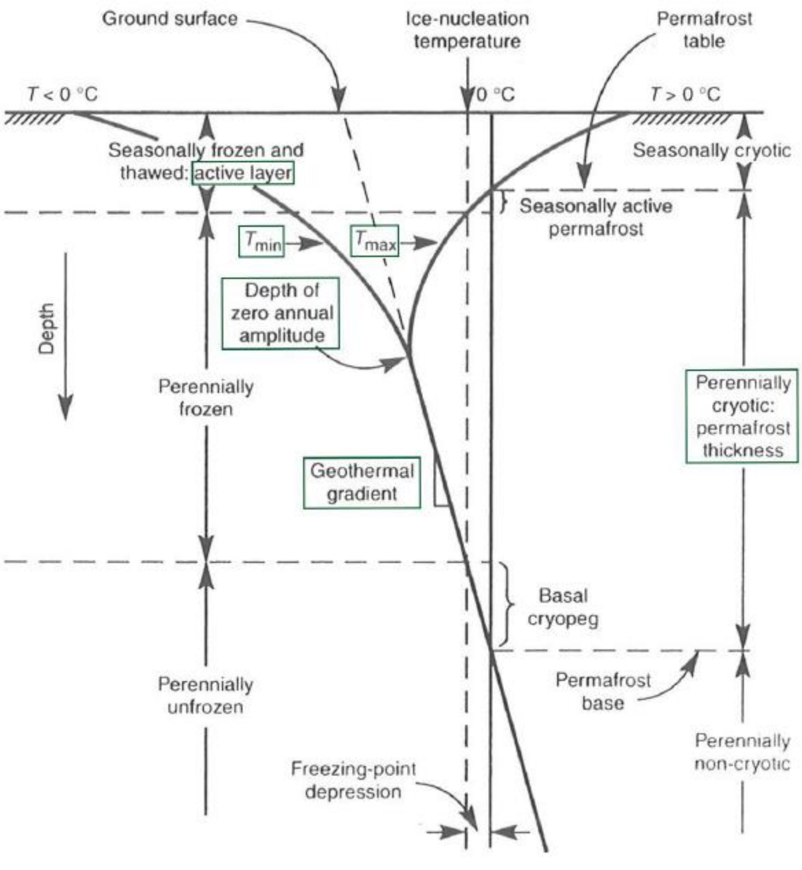

Figure 4: Schematic diagram of a trumpet curve with minimum, maximum and average permafrost temperatures and definitions (Strand, 2016).

As indicated in Figure 4, the active layer is the part of the soil where temperatures rises above 0 °C in summer. During autumn 2017 the thickness of the active layer measured at several research sites on Svalbard has been varying locally between 49 cm and 300 cm, but mainly between 100 cm and 200 cm (Christiansen et al., 2019). The hydrological regime as well as the activity of microorganisms in the active layer is very different from the permafrost layer, for example with respect to the ability of carbon decomposition. Zhang et al. (1998) emphasize an impact of the active layer thickness on the physical, chemical and biological features in the Arctic. The active layer depth does not only depend on the summer air temperature (Christiansen et al., 2010) but also on the thermal properties and the volumetric water content (Zhang et al., 1998).

2.2 Permafrost dynamic and latent heat release

After Roth et al. (2001), permafrost dynamics at Bayelva can be separated into four major stages, each corresponding to one season. In winter, the ground is completely frozen and often covered by snow. The volumetric water content of the soil is slowly decreasing over the whole winter and spring (compare Figure 5). In spring, snow is melting and meltwater is infiltrating into the top frozen layers of the ground. In summer, the active layer is thawing. The thaw front is often reaching its maximum depth in autumn. Areas close to the surface (4 cm) will thaw earlier than deeper areas (94 cm) (Figure 5). The ground heat flux (resulting from the surface energy balance) leads to thawing of the active layer. The heat is used in part to melt ground ice (latent heat), in part for evaporation (latent heat) and in part to warm the active layer (sensible heat). Latent heat consumption has a cooling effect on the surface (Roth et al., 2001). As a result, the soil temperature in one area might stay constant while the ice in the soil is melting. When the active layer is freezing back in autumn, there is an isothermal plateau during the freeze-back period (Roth et al., 2001). Water is converted back into ice, but during the process latent heat is released as thermal heat and keeps the soil at 0 °C for some time. This effect is also known as zero curtain effect (Roth et al., 2001).

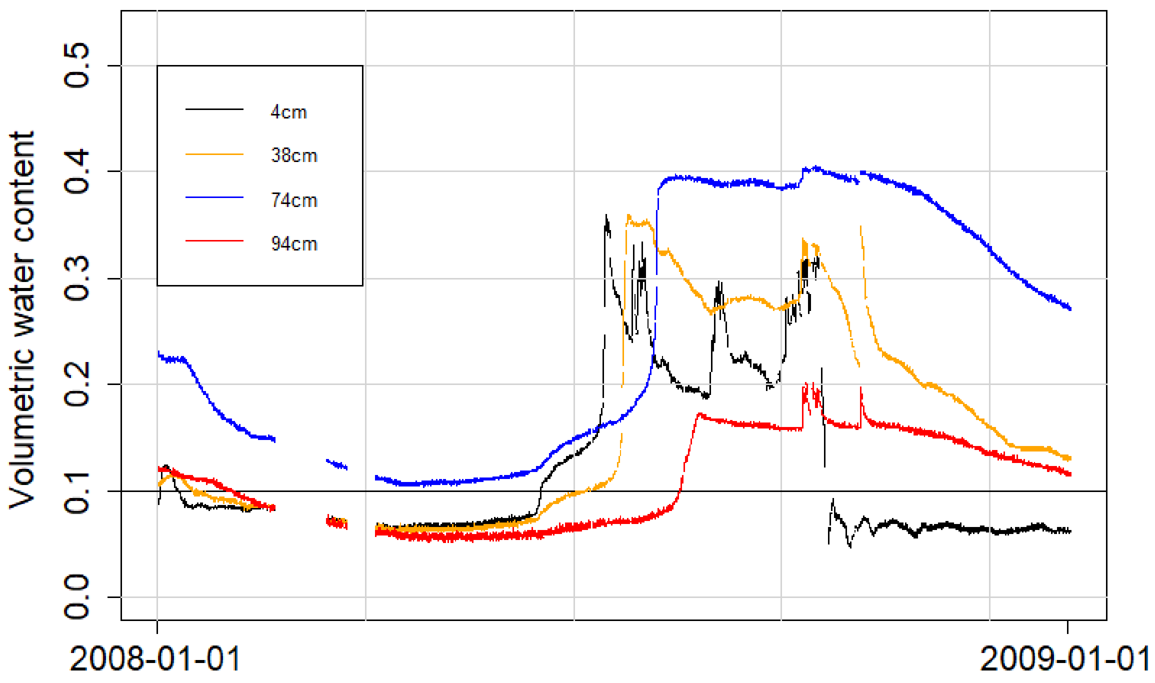

Figure 5: Evolution of the liquid volumetric water content in different depths over 1 year (2008 - 2009), data from Bayelva, 2008, 10% liquid volumetric water content marked as horizontal line for better orientation.

Snow in winter has a huge influence on the thermal regime of the permafrost. An increase in snow depth can lead to a warming of the permafrost due to the isolating properties of the snow (Romanovsky et al., 2010).

Strand (2016) notes for Svalbard that an increase of rain events on snow have happened as winter temperatures have risen. The rain percolates to the bottom of the snow cover and refreezes while the ground is warmed (sensible heat release) (Westermann et al., 2011). Hence, winter rain events have an effect on the snow properties and on the ground temperature.

In winter, pore water in the permafrost ground does not fully freeze. A thin water film often remains unfrozen between soil particles, due to adsorption (French, 2007). The finer the particles, the more liquid water the soil can adsorb. The profile in Figure 6 shows how much liquid water can be held in the pore spaces at each temperature of the ground in 22/23 cm at Bayelva, also referred to as freezing characteristic curve.

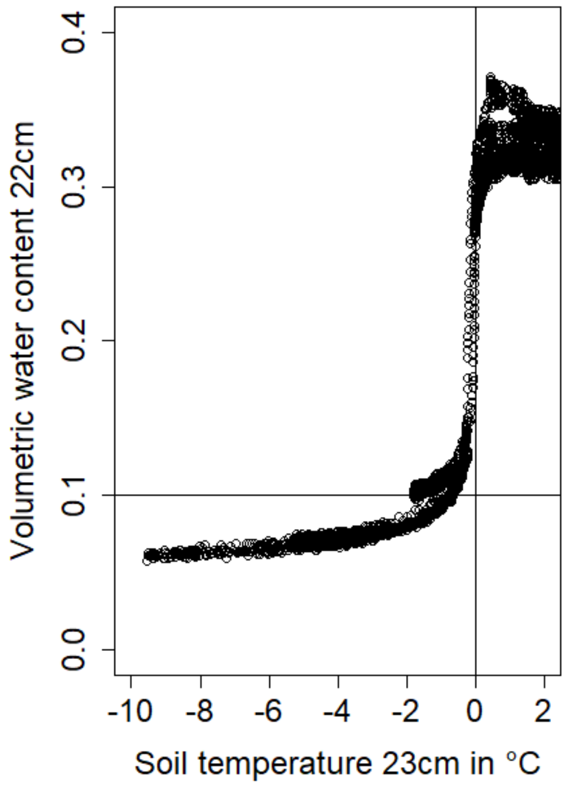

Figure 6: Liquid volumetric water content of the soil in 22cm depth depending on soil temperature in 23 cm depth, data from Bayelva, 2016.

3. Methodology

3.1 Data

The Bayelva dataset for air temperature, snow depth and liquid precipitation was obtained from PANGAEA (Boike et al., 2017 a). The data can be classified as level 1 data, meaning that the data was processed and quality flags were given to all data points (for flag system see Appendix A). The datasets temporal resolution for air temperature is 1 hour, from 1998 to 2009. However, from 2009 to 2018, it improved to 30 min. For the liquid precipitation the resolution was increased in mid- 2010 from 1 hour to 30 min. For the snow depth two values a day were measured from 1998 to mid- 2010. Afterwards, the frequency was increased to 1 value/ hour. The data from the first snow sensor (1999-2012) and the third (2013-2018) was combined.

As there is no soil station which was active over the whole time span of 20 years, the data from two stations was combined. The combined dataset is downloadable via PANGAEA as level 2 data (Boike et al., 2017b). The dataset includes soil temperature and LVWC data. Level 2 indicates that further processing has been done. During the process of combining both datasets, the data was not changed in any way, but the datasets of two stations were combined and the names of the parameters were changed (Appendix A). The soil stations were running simultaneously for 3 years and data was not differing much, hence the data combination was possible (Boike et al., 2017 b). Also, both stations are situated within a couple meters from each other (Figure 3). The resolution of the dataset is 1 hour.

The data obtained from the 9 m borehole at the Bayelva station can be downloaded from the Global Terrestrial Network for Permafrost (http://gtnpdatabase.org/boreholes/view/1192/). The dataset has a resolution of 1 value/hour from 2009 until 2018.

The data records at GTN-P and PANGAEA end in 2016 and 2017. Unpublished data from PD Dr. Julia Boike were used to complete all datasets with data until the end of 2018.

Boike et al. (2018) described which instruments and heights they use for the long-term measurements.

3.2 Quality assurance

The data was processed before by the working group of PD Dr Julia Boike and only data with good quality (Flag = 0) was used in this work (Appendix A). Data points with quality flags above 0 were excluded from this work. The dataset published on GTN-P is only including data of good quality although no flags are shown. The same is true for the level 2 dataset for the soil temperature and the LVWC. For the level 2 dataset only data with a good quality (Flag = 0) is published on PANGAEA.

For daily, monthly and annual means of the variables the calculation was only done, if a certain amount of data was available (Table 1).

Table 1: The amount of data which needs to be available for the execution of the daily, monthly and annual average calculation.

	Daily average	Monthly average	Annual average
Air temperature	>90%	>90%	>90%
Precipitation	>90%	>90%	>90%
Snow Depth	No restriction	>60%	Not calculated
LVWC	No restriction	>90%	>90%
Soil temperature	>90%	>90%	90%

As the air temperature is changing strongly over the day, at least 90 % of the hourly measurements had to be of good quality (Flag = 0); otherwise the daily average was not calculated. If 90 % of the daily measurements were available, then the monthly average was calculated. The same is true for the annual average. Since snow depth is not changing much within days, the average was always calculated. For the annual average calculation the calendar definition of a year (Jan - Dec) was taken.

3.3 Measurement variables

3.3.1 Air temperature

After downloading the data, daily, monthly and annual means of the air temperature record in 2 m heights were calculated. The mean annual air temperature trend was calculated using a linear least square regression in R (function lm(), version 1.1.456), which was used for all calculated trends in this work.

3.3.2 Liquid precipitation

The total daily, monthly, seasonal and annual liquid precipitation sums were calculated. Furthermore, an R Script was used to find the highest precipitation intensities per day. Spring was defined from March - May, summer from June - August, autumn from September - November and winter from December - February. The definition is following Hannsen- Bauer and Førland (1998).

3.3.3 Snow

Daily and monthly means were calculated. Using daily averages, the start date of the snow- covered period (snow depth >5 cm) and the end date (snow depth <5 cm) were determined. As there are negative values during summer in some years which might come from subsidence or measurement inaccuracies, the boundary of 5 cm was chosen. There might also be inaccuracies due to the slightly different settings of the combined snow sensors. Furthermore, the maximum snow depth in every year is listed below (Table 3).

3.3.4 Soil temperature and liquid volumetric water content

Daily, monthly and annual means of the soil temperature and the LVWC were calculated. Using the daily mean dataset, freezing and thawing times were determined manually. The thawing period in summer starts by the time the surface layer temperature becomes positive (>0 °C). The freeze-back period in autumn starts when the surface temperature is negative (<0 °C) but goes on until the whole active layer is frozen and its temperature below -1 °C. The time the soil is frozen is defined as the time span between the end of the freeze-back period (whole active layer is below -1 °C) and the day when the thawing starts (top of the soil >0 °C). Figure 6 shows that below a temperature of -1 °C the volumetric liquid water content is still decreasing, which indicates an ongoing of the refreezing, but only slightly. Hence, the boundary of -1 °C was chosen for the state frozen/unfrozen.

For the 9 m borehole annual temperature maxima, minima and annual means were calculated for each depth. With the resulting trumpet curve, active layer depths were estimated, whereby an inaccuracy of +/- 0.1 °C of the sensor was considered.

The idea was to look into specific months and see how much the LVWC and the soil temperature changed in these months over the 20 years. Is there a higher increase in winter months such as February than in summer months such as July? For each month separate trends for the increase/ decrease of the LVWC and the soil temperature over the 20 year period were calculated. There are several trends for each month as there are several depths for which trends were calculated. A t-test was used for evaluating the significance of the trends with α= 0.05. The months with the most interesting results were analysed further using a correlation analysis. The Pearson correlation coefficient was taken for the correlation analysis. In the correlation analysis next to the soil temperature and the LVWC from the month, variables such as mean air temperature, liquid precipitation sum and mean snow depth from the month were used, as well as the liquid precipitation sum from the previous month and the freezing back and thawing dates (Appendix F).

4. Results

4.1 Climate characteristics

For the 20 year period 1998-2018 general climate parameters were determined. A mean air temperature of -4.2 °C was calculated for the period. In comparison, Førland et al. (2011) calculated a mean air temperature of -6.3 °C for the period 1961 - 1990 for Ny-Ålesund. Within the analysed period 1998 - 2018 an increase of +1.46 °C (+/- 0.05 °C) per decade is displayed (Figure 7). The highest annual mean was calculated in 2016 with -1.6 °C and the lowest in 2003 with -7.2 °C.

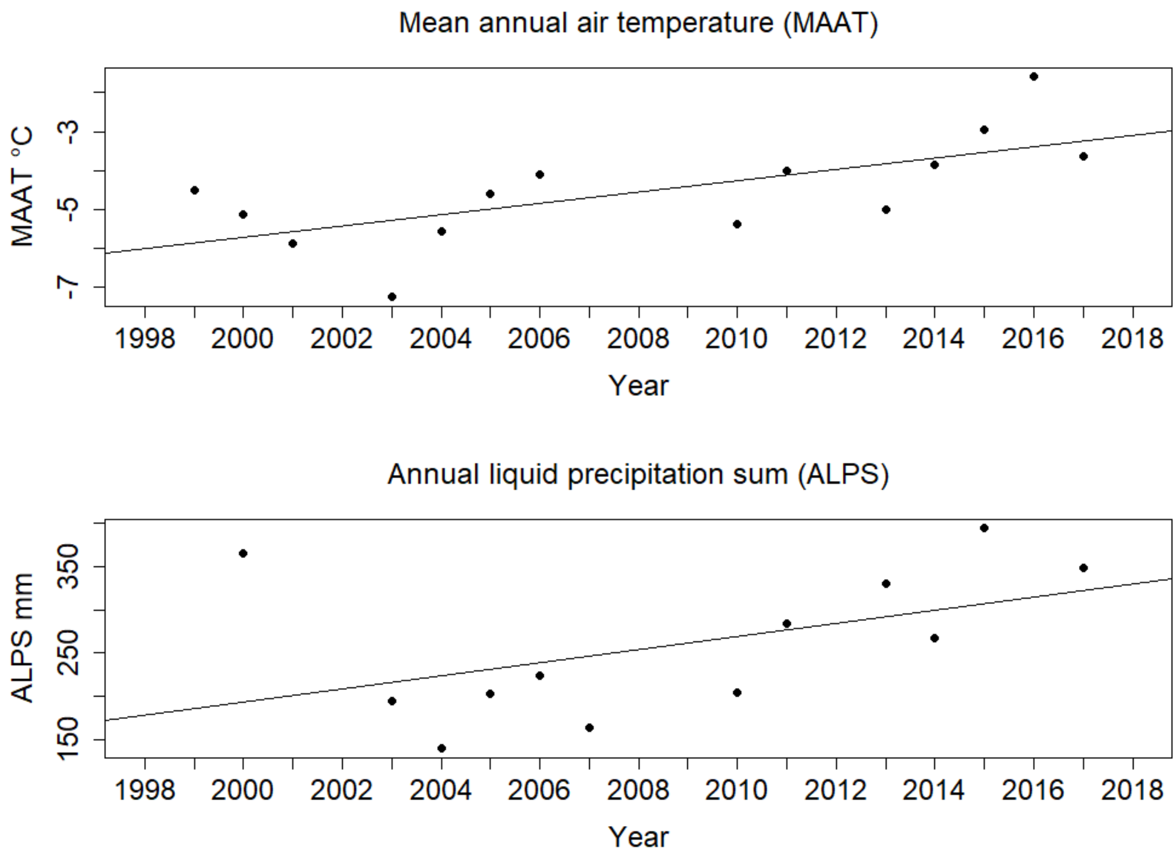

Figure 7: Annual trends derived from annual average data of the air temperature (R^2= 0.45) and from annual sums of liquid precipitation (R^2= 0.23) for the data measured at Bayelva. Years in which less than 90 % of the monthly averages were available were excluded.

The annual liquid precipitation is varying strongly over the years (Figure 7). The highest annual precipitation rate was measured in 2015 with 394.1 mm, the lowest in 2004 with 139.1 mm. An increase of 76mm (+/- 44 mm) per decade was calculated. Førland et al. (2011) stated an annual average precipitation (total) of 385 mm for the period 1961-1990 at Ny-Ålesund.

For the seasonal precipitation, a seasonal average was calculated (Table 2). In comparison to Førland and Hanssen- Bauer's study (2000) which measured total precipitation at Ny-Ålesund, this study uses liquid precipitation only. For the exact values of each year see Appendix B.

Table 2: Seasonal Precipitation. Left: Mean seasonal precipitation calculated with data from Bayelva (1998-2018); Right: Mean Total Precipitation in Førland and Hanssen- Bauer (2000) for period 1961-1990.

	Mean Liquid Precipitation for Period **1998-2018** (mm)	Mean Total Precipitation Førland and Hanssen- Bauer (2000) for the period **1961-1990** (mm)
Spring (MAM)	28.4	77
Summer (JJA)	87.7	88
Autumn (SON)	113.5	115
Winter (DJF)	53.2	90

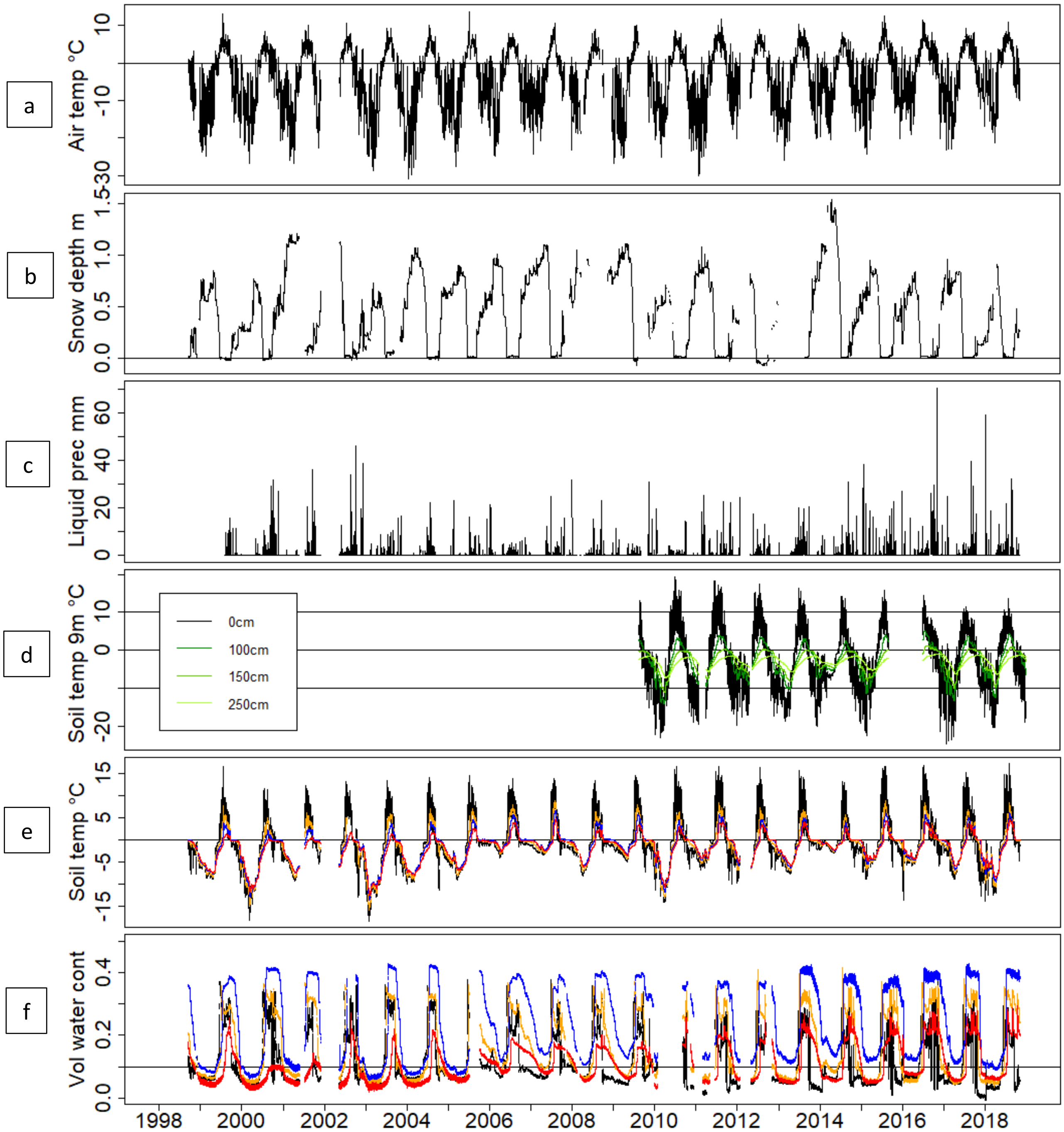

Figure 8: Overview over all climate variables and subsurface characteristics at Bayelva over the time span of 20 years with a) daily average of the air temperature measured in 2 m in °C, b) daily average data of the snow depth in m including subsidence in summer, c) sum of liquid precipitation per day in mm/day, d) hourly soil temperature from the 9 m borehole, e) hourly soil temperature in different depths: black= 4cm, orange= 38cm, blue= 74cm and red= 94cm depth from the soil profile and f) hourly liquid volumetric water content measured at the soil profile in decimal numbers at the same depth as e).

4.1.1 Liquid precipitation intensity

The highest liquid precipitation/ day events which occurred during the 20 years are listed in the table below. The table shows that the highest rain intensities per day were measured from the end of August until mid- January. During late summer/ autumn the active layer is often quite destabilized. Rain events can therefore trigger mudflows. Some of the events might fall under the definition of rain on snow events. If water enters the soil in autumn and winter, it may influence the water content of the soil.

Table 3: Ranking of 1st-10th maximum day precipitation event from 1998 to 2018. Middle column: day of the event, right column: Sum of liquid precipitation in mm/ day.

Ranking	Date	Max Day Precipitation mm/ day
1	07.11.2016	70.3
2	13.01.2018	59.2
3	08.10.2002	46.1
4	09.10.2002	44.2
5	03.09.2017	39.4
6	07.12.2002	38.5
7	23.01.2015	38.2
8	18.09.2001	35.8
9	25.08.2002	33.8
10	30.08.2018	32.2

4.1.2 Maximum snow depth

The absolute maximum of snow depth is also varying strongly among the years, with the highest value 155 cm measured in winter 2013/2014 and the lowest maximum 72 cm measured in the winter 2002/2003 (Table 4). The table and Figure 9 are showing the maximum snow depth for winters with enough data, derived from daily averages. From the available years no clear trend is visible (Figure 9).

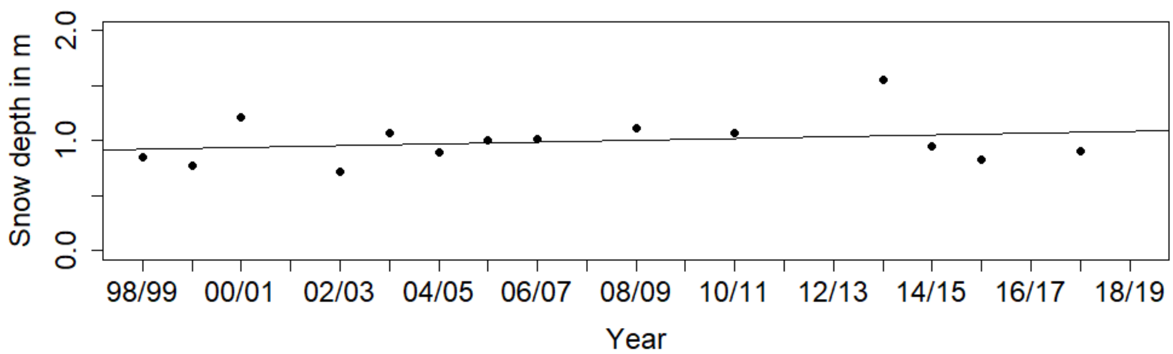

Figure 9: Maximum snow depth in m occurring in each winter with trend derived from daily mean snow depth data.

Table 4: Maximum snow depths measured in each winter with right column: winter period, second right: date of the snow maxima, second left: max snow depth in cm at the date and left: additional comments on data gaps.

Winter	Date of Maximum	Max Snow Depth (cm)	Comments
98/99	27/04/1999	85	
99/00	12/04/2000	77	
00/01	30/04/2001	121	No data in May
01/02	-	-	
02/03	07/03/2003	72	
03/04	15/03/2004	107	
04/05	31/03/2005	89	
05/06	11/03/2006	100	
06/07	24/04/2007	101	5 days missing after 24/4/2007
07/08	-	-	
08/09	28/04/2009	111	
09/10	-	-	
10/11	21/02/2011	107	
11/12	-	-	
12/13	-	-	
13/14	15/04/2014	155	Some days missing in March
14/15	26/03/2015	95	
15/16	24/04/2016	83	
16/17	-	-	
17/18	23/04/2018	90	Some days in March and April missing

4.1.3 Duration of snow cover

The duration of the snow cover has shortened since 1998 (Figure 10). Over the 20 year period, the onset of the snow deposition was delayed while the end of snow happened earlier. Still, the fluctuation is very high and the coefficient of determination for both trends is low. The snow deposition tends to be 14 days later every decade (+/- 10 days) (Figure 10 a) and the end of snow happens 8 days earlier (+/- 5 days) (Figure 10 b).

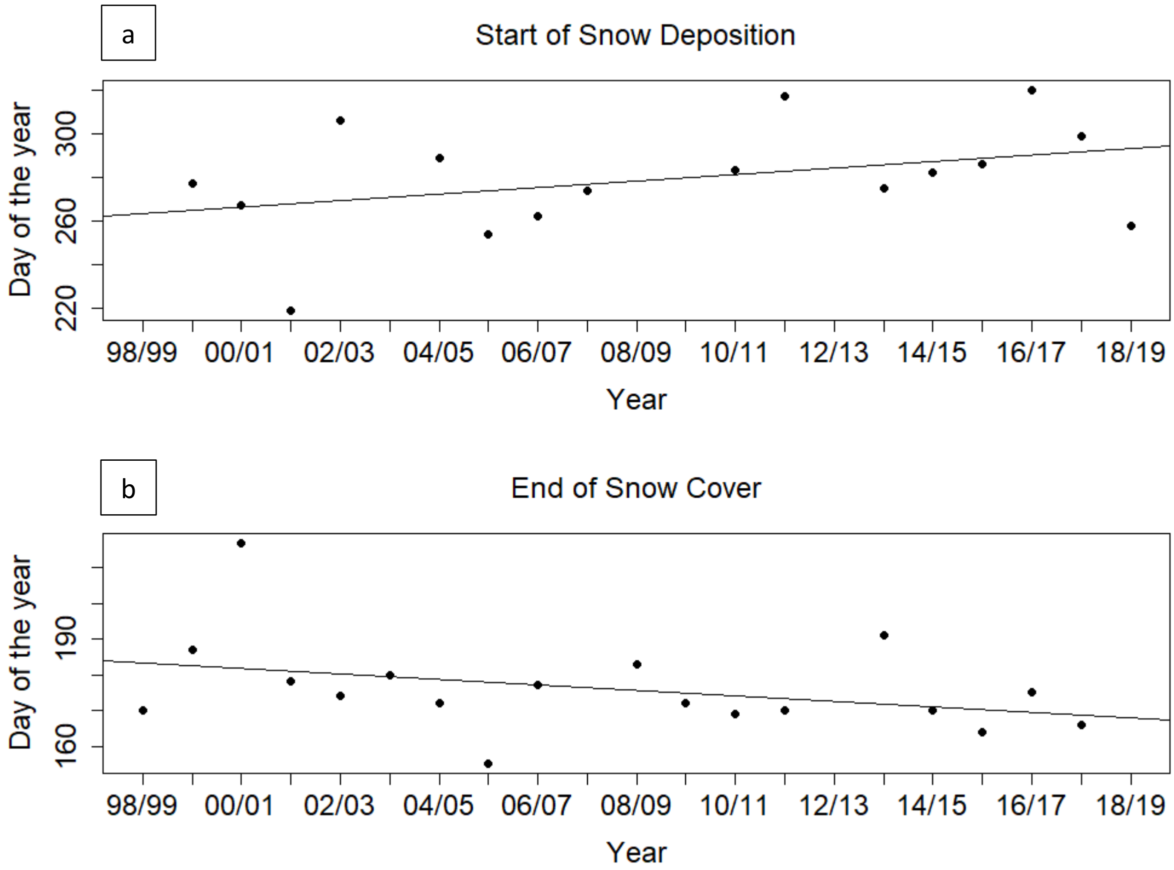

Figure 10: Key graph snow dynamic changes. a) Start date of the snow deposition every year with trend (R^2=0.14); b) End date of the snow cover every year with trend (R^2=0.13). For both graphs the daily average dataset was used.

4.2 Soil temperature and liquid volumetric water content

4.2.1 Active layer thickness

The data used in this section comes from the 9 m borehole (hourly values) which has an uncertainty of +/- 0.1 °C. In 2010, the thaw depth did not extend beyond 1.5 m (-0.12 °C in 1.5 m). In 2015 the active layer was deeper than 1.5m (0.25 °C in 1.5 m). In the years between 2010 and 2015 the active layer was sometimes above or below 1.5 m, but mainly deeper than 1.5m (Figure 8 c blue line). After 2015 the temperature in 1.5m depth always reached above 0°C in summer. According to Ebenhoch (2018), the active layer reached the 2 m boundary in 2016 for the first time, calculated with the help of the Stefan model.

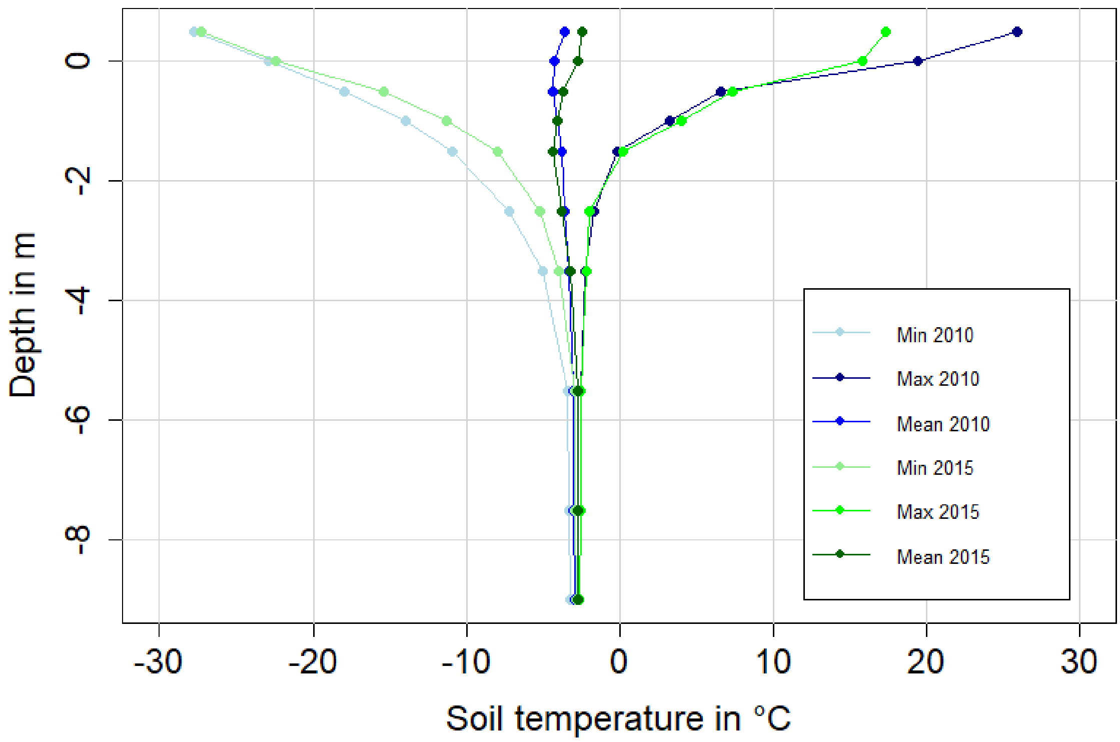

Figure 11: Trumpet curves for years 2010 & 2015 from soil temperature data (°C) with hourly resolution from the 9m deep borehole at Bayelva.

4.2.2 Freeze-back and thaw period

The timespan when the soil is completely frozen has decreased since 1998 for about 31 days per decade (Figure 12 a and Table 5). The period is defined as the time between the end of the freeze-back period and the thawing date (for definitions see Chapter 3.3.4). This is due to the earlier thawing of the soil in summer (Figure 12 e) and the delay of the date when the soil is completely frozen back (end of freeze-back period) (Figure 12 c). In 1998, the soil refroze (below -1 °C) in November, but in some years it can also take until March until the soil is entirely refrozen (see for example 2005/06, Figure 12 c). The thawing period started in mid- June in recent years, instead of late June or July as 20 years ago. The start of the freeze-back period is delayed as well. It may take until November in recent years until it starts, while it started in mid- September in the late 90s.

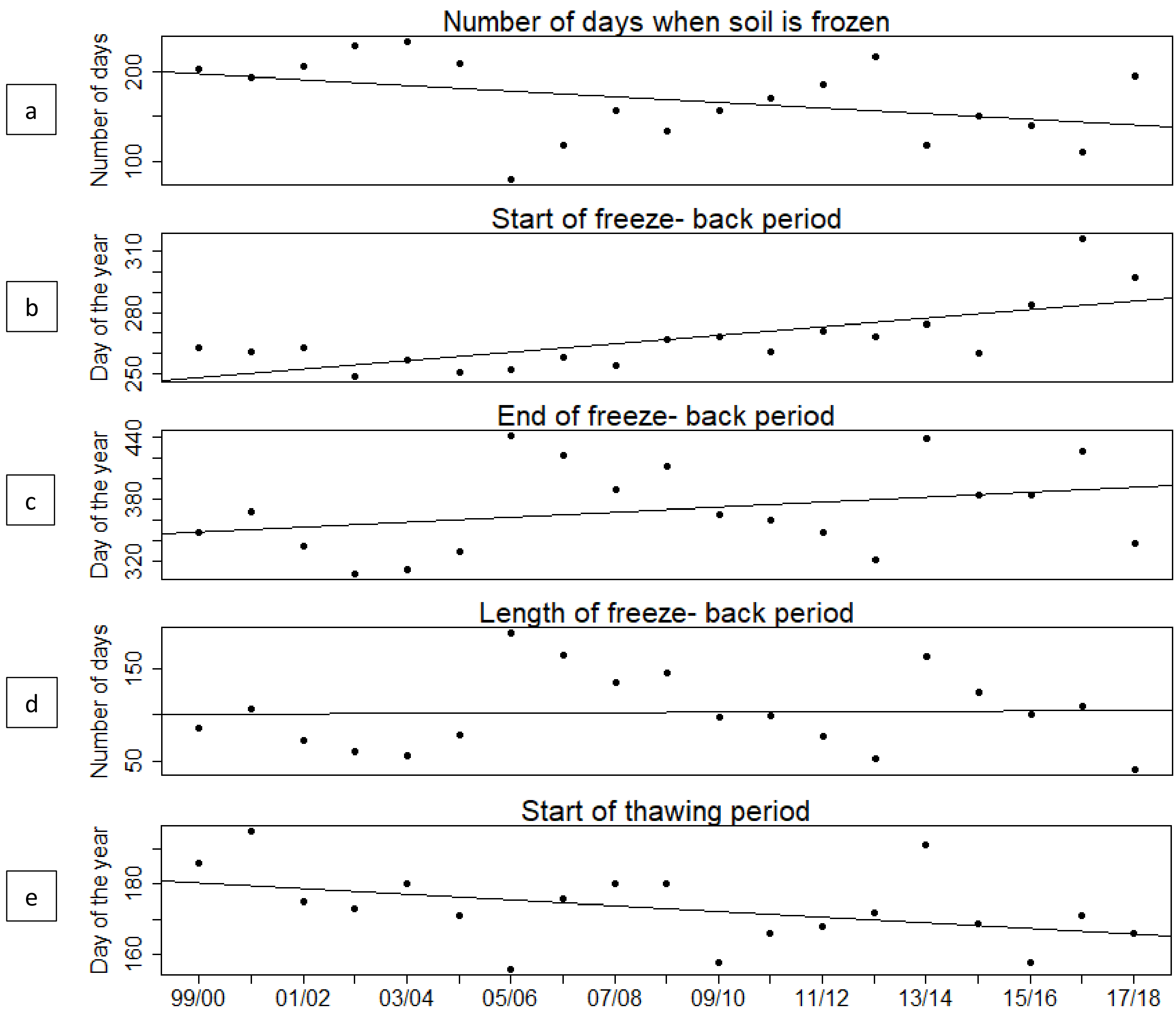

Figure 12: Freezing times and thawing times with trends determined from daily average data of the soil temperature from all depths of the soil profile. a) Number of days when the soil is frozen in each winter; b) start date of the freeze-back as day of the year; c) end of the freeze-back period as day of the year; d) the length of the freeze-back period equals the difference between start and end of the freeze-back period; e) start of thawing in the following summer (as day of the year including the start of the next year).

Table 5: Slope and standard error to trends of Figure 12. Red marked are trends which are significant (α= 0.05).

	Slope in days/ year	standard error in days/ year
a) Number of days when the soil is completely frozen	-3.13	1.74
b) Start of freeze-back period	2.09	0.51
c) End of freeze-back period	2.33	1.75
d) Length of freeze-back period	0.24	1.80
e) Start of thawing period	-0.81	0.41

4.2.3. Warming and wetting of the active layer

The annual average for the soil temperature has increased in a range of 0.9 °C and 1.6 °C (+/- 0.6 °C) per decade, whereby the range comes from the different increases in the different depths 4cm to 133cm (Figure 13 a). The trends were analysed for every depth separately and all results and uncertainties can be found in the Appendix C. In deeper layers the increase in soil temperature was slightly higher than in shallower layers (Figure 13 a).

The LVWC has overall increased as well. For the depths 10 cm – 94 cm the increase was ranging in the depths between 0.65 % and 3.2 % (+/- 1.2 %) per decade. The trend was higher in deeper layers than at shallower depths (Figure 13 b). At the surface at 4 cm though, the LVWC declined about - 1.7 % per decade. In winter the LVWC stayed partly (in 74 cm depth) above 10 % (Figure 8 f, blue line).

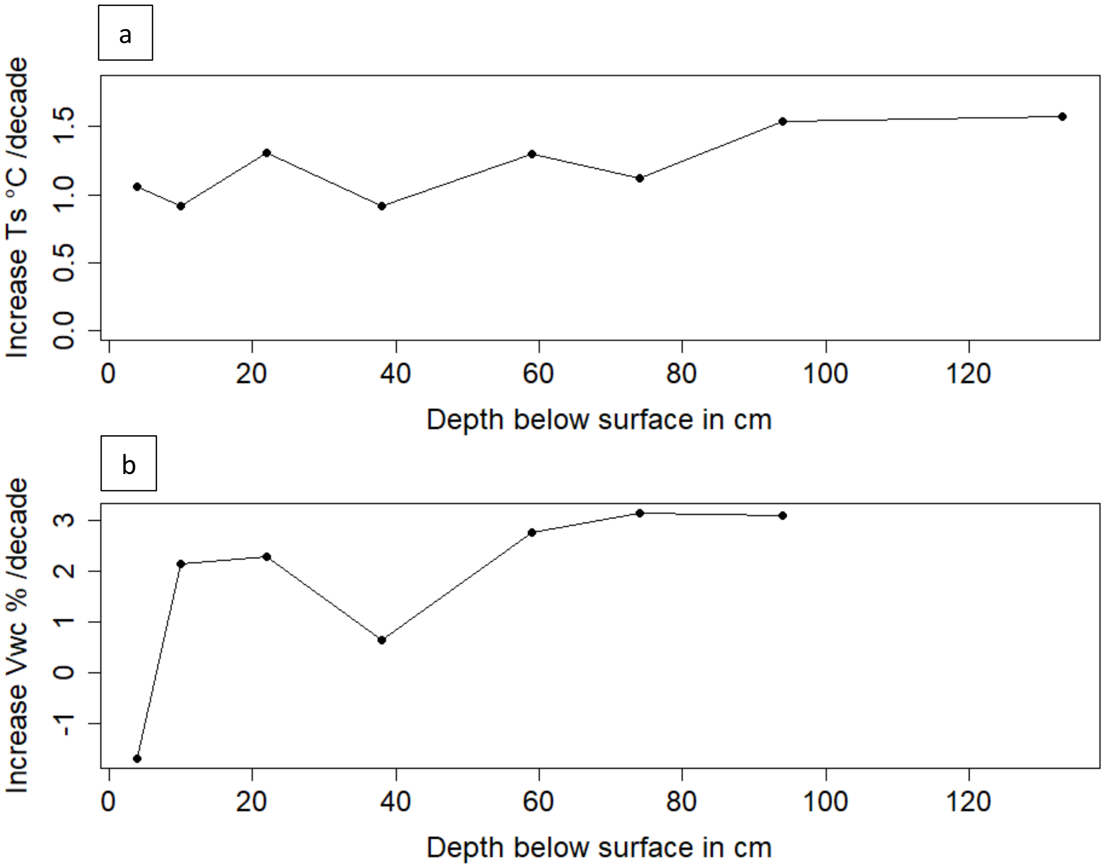

Figure 13: Changing subsurface conditions. a) Increase in soil temperature in °C per decade for several depths based on annual average data. b) Increase in liquid volumetric water content in % per decade for several depths based on annual average data.

To answer the question, whether the increase of the soil temperature and the LVWC is varying between seasons over the 20 year period, the trend calculation was made for only one month at a time. For example the monthly averages from October from the 20 years were analysed for trends and are shown as an example in the Appendix D.

Overall the trends for the soil temperature and the LVWC were positive in all months (Figure 14). Only the LVWC in 4 cm depth shows a decline almost constantly throughout the months. All results from all months can be found in the Appendix E. For the analysis a significance threshold of $\alpha = 0.05$ was taken.

Of all months, the month October shows the greatest increase in the LVWC throughout the depths with a maximum of +7.1 % per decade in 22 cm depth, whereby most trends are significant (Appendix E). The highest decline in surface LVWC can be found in July with - 4.7 % per decade. In February, there is the highest increase in the soil temperature but here the trends are not significant (Appendix E).

In the following, the months October, February, April and July will be discussed and analysed further. After the definition of Hanssen- Bauer and Førland (1998) one month of each season was taken into account. As discussed above, October, July and February show the greatest changes. In April, the maximum snow depth is reached in almost all years, which makes the month interesting to look at.

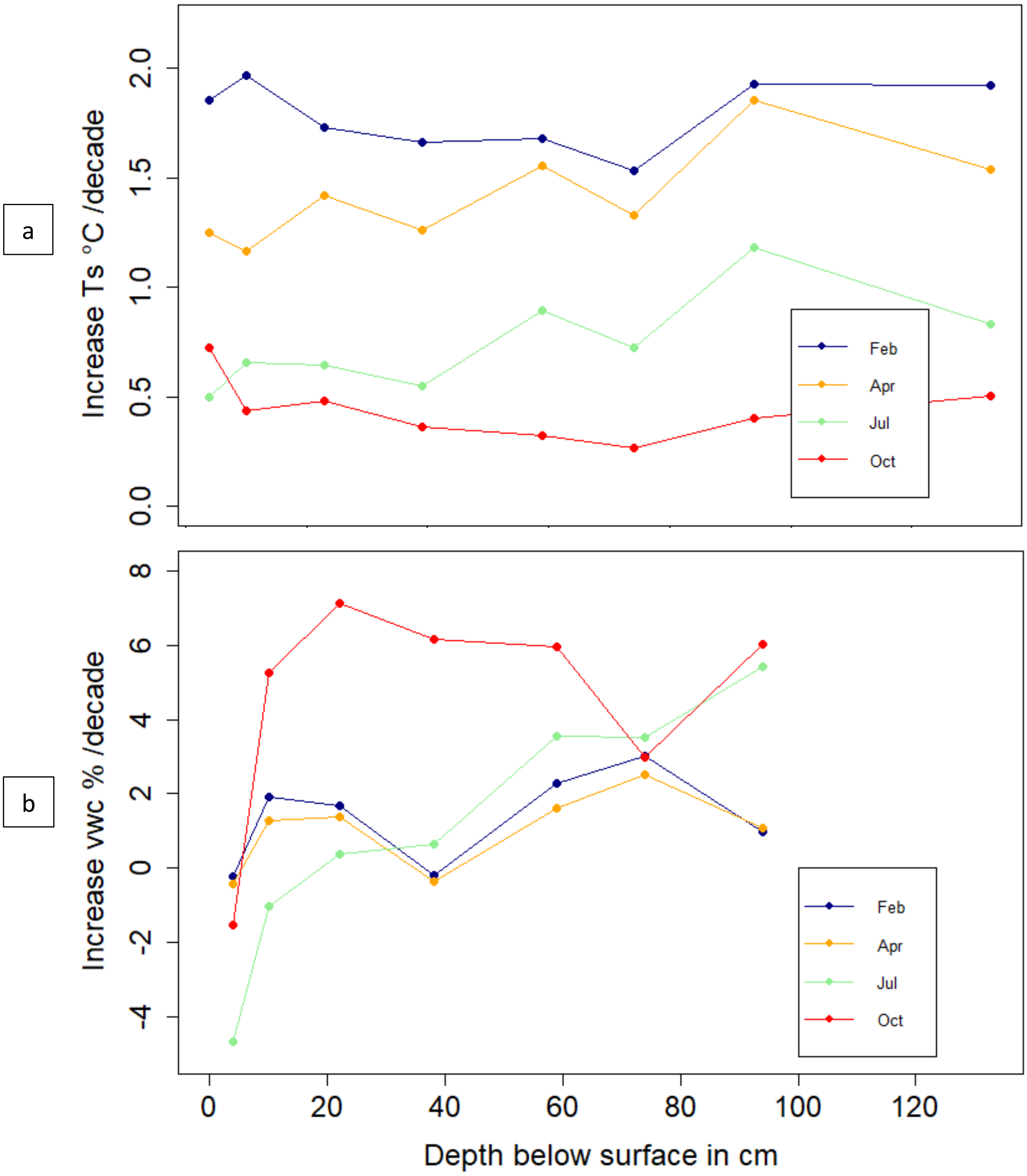

Figure 14: Soil temperature and liquid volumetric water content change per decade for several months in various depths. a) Soil temperature increase in °C per decade calculated for the months February, April, July and October for various depths from monthly average data. b) Liquid volumetric water content increase in % per decade calculated for the months February, April, July and October for various depths from monthly average data.

Further statistical methods were applied to determine variables which correlate with the changes of the soil temperature and the LVWC in the specific months. All parameters available were plotted against each other to analyse their correlation (Pearson correlation coefficient). The results are displayed in a correlation matrix for each month (Appendix F). The results with the highest correlation are shown below.

For the month **October,** the correlation between the start of the freeze-back period and the soil temperature and the LVWC was the highest (Figure 15 a & 15 b). The depth used and shown in Figure 15 a & 15 b is 94 cm. The correlation is varying strongly in between the depths.

For **February,** the LVWC and the soil temperature are negatively correlated with the time length of the soil frozen (Figure 15 c & 15 d). The shorter the period when the soil is frozen (under -1 °C) the higher are the LVWC and the soil temperature in February. The correlation coefficient was almost equal for all depths, just slightly smaller for the soil temperature in the first 10 cm, where other parameters may have a stronger influence.

For **April,** the main correlation variable of soil temperature and LVWC is the length of the period when the soil is frozen. The longer the soil stays under -1 °C, the lower the soil temperature and the LVWC are in April (Figure 16 a & 16 b). Still, the correlation of the parameters is weaker than in February. The correlation is stronger for deeper depths than for shallow areas (>10 cm). Especially for the LVWC in 4 cm depth the regression coefficient was low as the layer is getting drier.

In **July,** the soil temperature and the LVWC are primarily correlating with the end of snow cover date (Figure 16 c & 16 d). The earlier the snow is melting, the wetter and warmer the ground is in July. As the snow is isolating the ground and limiting the exchange between ground and air, the disappearance of the snow is important. The correlation is weak for the LVWC in the first 40 cm, probably due to the decrease of the LVWC in the top layers (Figure 14 b).

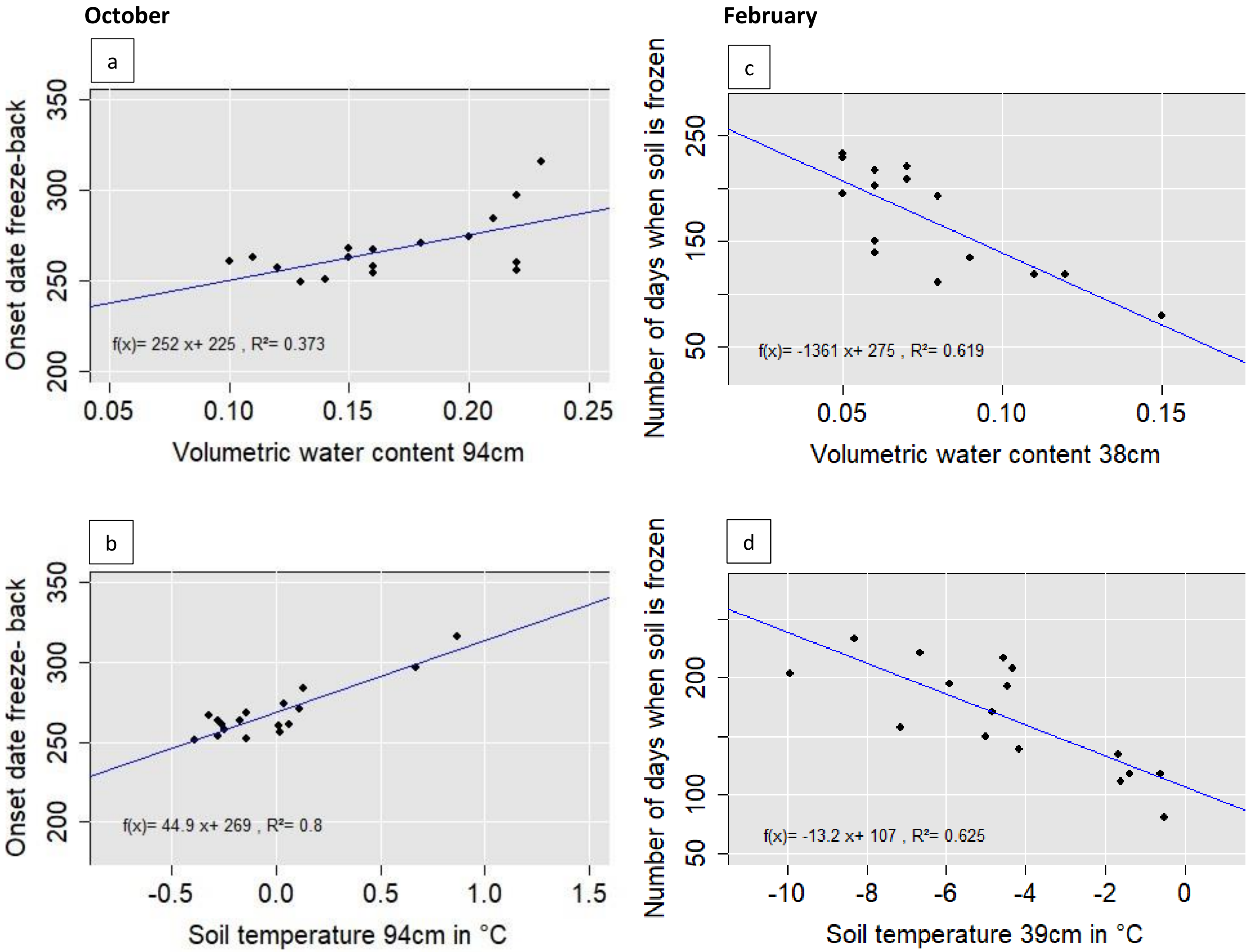

Figure 15: Monthly means of the soil temperature and the volumetric water content from the months October and February: a) Soil temperature (94cm) in October in °C in correspondence with the start date of the freeze-in period, b) Volumetric water content (94cm) in October in decimal numbers in correspondence with the start data of the freeze-in period, c) Soil temperature (39cm) in February in correspondence with the number of days when the soil is frozen, d) Volumetric Water content (38cm) in February in correspondence to the number of days when the soil is frozen. 95% confidence interval is displayed as grey shading. f(x) as formula of the linear model is used and R^2 as regression coefficient.

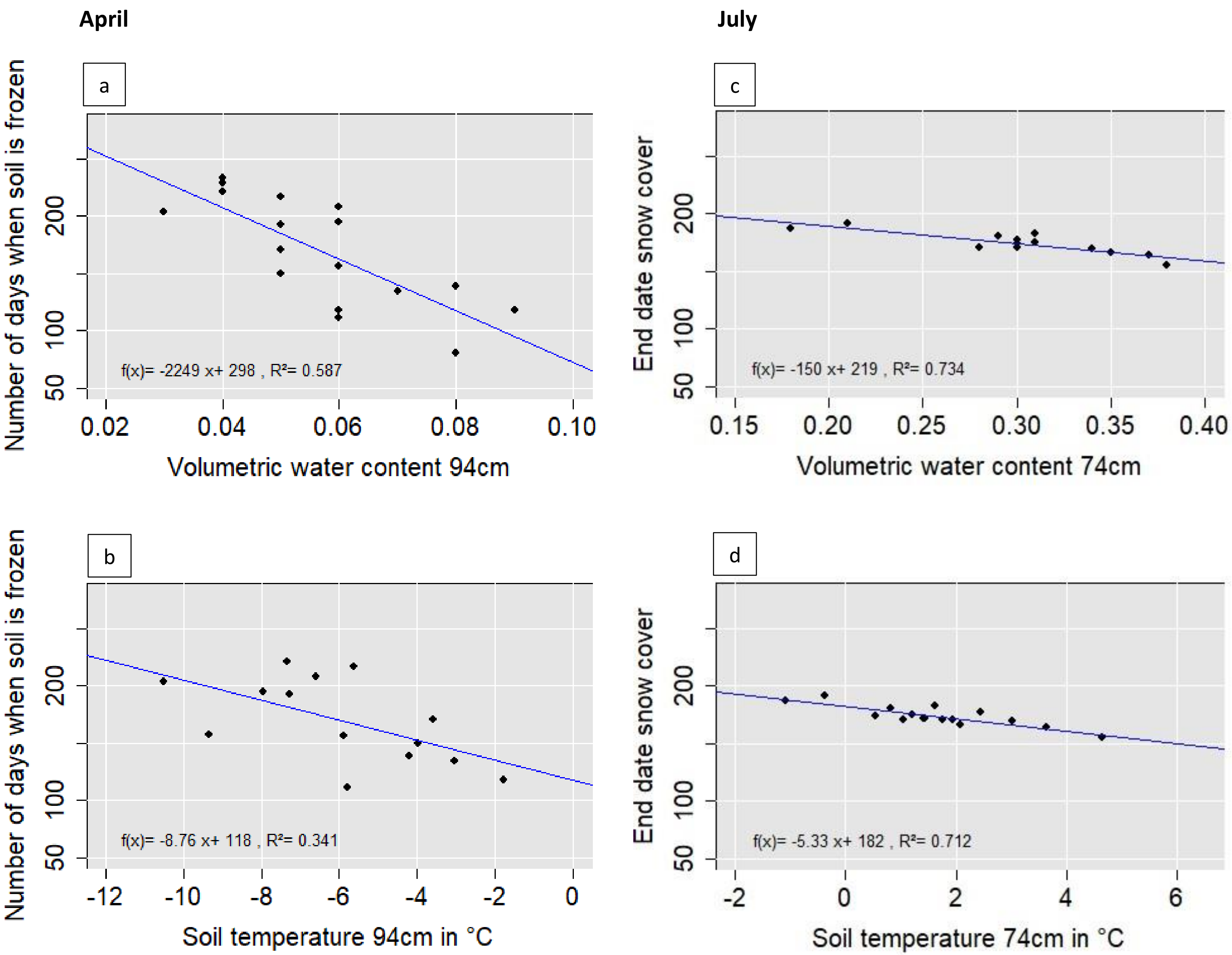

Figure 16: Monthly means of the soil temperature and the liquid volumetric water content from the months April and July : a) Liquid volumetric water content (94 cm) in decimal numbers in April in correlation to the number of days when the soil is frozen, b) soil temperature (94 cm) in °C in April in correlation to the number of days when the soil is frozen, c) liquid volumetric water content (74 cm) in decimal numbers in July in correlation to the end of the snow cover date as day of the year (DOTY), d) soil temperature (74 cm) in °C in July in correlation to the end of snow cover date as DOTY. f(x) as formula of the linear model is used and R^2 as regression coefficient.

5. Discussion

5.1 Air Temperature

The results show that the air temperature has increased by 1.46 °C (+/- 0.05 °C) per decade in the past 20 years. Similar trends for slightly different periods were calculated by Ebenhoch (2018) with 1.4 °C per decade for Bayelva and by Maturelli et al. (2015) with +1.3 K (+/- 0.7 K) per decade for the AWIPEV station in Ny-Ålesund. Rinke et al. (2017) found an increase in extreme cyclone events on Svalbard in winter, which are associated with heat and moisture transport into the Arctic. The cyclone activity is again related to sea- ice and atmospheric circulation changes (Rinke et al., 2017).

As stated above, the parameter air temperature has a strong influence on the ground as it is the primary factor influencing the thermal regime of the ground. In the correlation analysis air temperature often reached high values, but was not the primary correlation factor (Appendix F).

5.2 Liquid precipitation

The amount of rain has increased over the past 20 years by 76 mm (+/- 44mm) per decade. Next to extreme cyclone events, sea ice changes can be responsible for more rain as the winds can take up more water from the ocean and bring humid air in if the sea ice is formed later. The results give supporting evidence for the hypothesis that the rain pattern changed. Especially in autumn and winter the rain was partly falling with very high intensity (Table 3).

Though, the increase in the annual liquid precipitation might be also due to more snow falling as rain, meaning that the total precipitation could be still the same.

Regarding the instruments, conditions can be harsh and data gaps (data points from 6 of 18 years are missing; Figure 7) occur. Calculated trends are often highly uncertain as there are just few measured points (<20 sampling points). With a longer data series, the uncertainty of the annual increase of liquid precipitation could be reduced.

Rain might have an impact on the freezing period. The results indicate that the more rain there is in autumn, the later the freezing period starts. This is due to the fact that rain will add additional water to the ground, which as turned into ice releases energy and stabilize the ground temperature.

5.3 Snow

The study shows that the maximum thickness of the snow cover has not evidently changed over the 20 year period. The snow cover is vanishing earlier in summer, whereas the ground can heat up earlier and for a longer time span and the active layer can thaw earlier and longer. The earlier end of the snow cover was also the primary correlation factor for the soil temperature and the LVWC increase in Bayelva in July. With the earlier thawing and the deepening of the active layer, the deeper zones of the active layer are not as frozen anymore as 20 years ago. The snow cover is also very much influenced by air temperature and by precipitation.

The findings of this work fit to Bilt et al. (2019) projections for Svalbard which forecast an increased mean annual air temperature, increased annual precipitation and shorter snow cover periods for the future in reference to 1971-2000.

The earlier melt of the snow cover may have caused the drying of the top layers of the active layer in summer. The time when the snow melts and the evapotranspiration rate are strongly dependent on the air temperature.

5.4 Liquid volumetric water content and soil temperature

The LVWC and the soil temperature have increased over the past 20 years. While the LVWC declined in the first 4 cm of the ground, it rose between 10 cm and 94 cm depth. Probably the effect can also be seen in deeper zones as the active layer has thickened to more than 150 cm, but no deeper measurements from the two soil stations are available. The active layer thickness measured at the Ny-Ålesund station from the Insubria University in 2016/17 fits with 192 cm to the results from Bayelva (Christiansen et al., 2019). Generally, greater LVWC can also counteract the thawing of the ground (Nikolsky and Romanovsky, 2018) and hence counteract the active layer deepening.

The highest increase in the LVWC can be found in October as the soil is freezing back later as it did 20 years ago. 20 years ago, the freeze-back started in mid- September, in recent years in October. In the correlation analysis, the increase in soil temperature and LVWC in October was primarily corresponding with the start date of the freeze-back. In February and April the changes were mainly corresponding with the length of the period when the soil is frozen. As the number of days when the soil is frozen is declining, the active layer does not have the same amount of time anymore to cool down and turn the liquid water into ice. There is an increase in LVWC, but especially for February the strongest increase in soil temperature is shown. In August when the active layer is mainly unfrozen, the increase in LVWC can also come from more precipitation. The deepening of the active layer can cause a lowering of the water table and hence, the drying of the soil surface over the whole year could be explained. Evapotranspiration might also play a role in summer and explain the strong decrease of -4.7 % per decade in surface volumetric water content in July.

The increase in soil temperature and LVWC was generally higher and more significant in deeper zones of the active layer than in shallower zones.

The correlation analysis cannot give answers to what caused the increase of the LVWC and the soil temperature. Hence, more advanced statistical methods could be applied to find the primary reason for the change. Furthermore, water budget calculations could give an indication. Also, more explanatory variables could be used in the correlation analysis.

As layers of the ground (around 74 cm depth) partly contained more than 10 % LVWC in winter, the question arises whether the ground was really freezing back in winter. Based on the freezing characteristic curve (Figure 6) the -1 °C boundary was chosen for the definition of frozen. Following this definition, the soil was freezing back each year but the LVWC of >10 % shows a storage of energy in the soil over winter which cannot leave the ground.

The calculated trends seem partly quite strong, for example the number of days when the soil is frozen declined with a trend of -31 days per decade (+/- 17 days). The years 2005-2008 were very warm and moist years. Due to these peaks in the middle of the dataseries, the trends are quite uncertain.

6. Conclusion

Climate and soil variables changed greatly over the past 20 years at the site Bayelva in north- west Svalbard. While air temperature and liquid precipitation increased, snow cover length and the period when the soil is frozen shortened. Therefore, the active layer at the site has been deepening, wetting and warming substantially. As the air temperature is projected to rise further in the future, further changes in the precipitation regime, the freezing period and the subsurface conditions can be expected. The changes in the soil regime will affect biochemical fluxes such as the decomposition of organic carbon by microorganisms which is enhanced under wetter and warmer conditions.

Acknowledgements

A big thanks goes to the SPARC working group, who offered me a great working spot, gave me access to datasets and supported me throughout the working process.

Julia Boike and Axel Bronstert I thank for their willingness to support my thesis. In particular I would like to thank Julia Boike for her patience in answering my emerging questions, guiding me through my work at a good pace and always giving me advice when I did not know any better and Inge Grünberg for helping me out whenever it was needed and giving me very helpful feedback. I would also like to acknowledge Toni Schmidt for providing advice and R scripts, Stephan Lange for helping me with R, Jan Nitzbon for providing feedback and Lena Nicola for her never ending support.

References

ACIA (2004). *Impacts of a Warming Arctic: Arctic Climate Impact Assessment.* Available at: https://www.amap.no/documents/doc/impacts-of-a-warming-arctic-2004/786 (Accessed: 20 April 2019).

Boike, J., Juszak, I., Lange, S., Chadburn, S., Burke, E. J., Overduin, P. P., Roth, K., Ippisch, O., Bornemann, N., Stern, L., Gouttevin, I., Hauber, E., Westermann, S. (2017a). 'Meteorological data at station Bayelva (1998-2017, level 1, version 1), link to archive: PANGAEA, https://doi.org/10.1594/PANGAEA.882058.

Boike, J., Juszak, I., Lange, S., Chadburn, S., Burke, E. J., Overduin, P. P., Roth, K., Ippisch, O., Bornemann, N., Stern, L., Gouttevin, I., Hauber, E., Westermann, S. (2017b). 'Soil data at station Bayelva (1998-2017, level 2, version 1), link to archive: PANGAEA, https://doi.org/10.1594/PANGAEA.882061.

Boike, J., Juszak, I., Lange, S., Chadburn, S., Burke, E., Overduin, P.P., Roth, K., Ippisch, O., Bornemann, N., Stern, L., Gouttevin, I., Hauber, E. and Westermann, S. (2018). 'A 20-year record (1998-2017) of permafrost, active layer and meteorological conditions at a high Arctic permafrost research site (Bayelva, Spitsbergen)', *Earth Syst. Sci. Data,* 10 (1), pp. 355–390, doi: 10.5194/essd-10-355-2018.

Cannone, N., Guglielmin, M. and Gerdol, R. (2004). 'Relationships between vegetation patterns and periglacial landforms in northwestern Svalbard', *Polar Biol.*, 27, pp. 562-571.

Christiansen, H.H., Etzelmüller, B., Isaksen, K., Juliussen, H., Farbrot, H., Humlum, O., Johansson, M., Ingeman Nielsen, T., Kristensen, L., Hjort, J., Holmlund, P., Sannel, A.B.K., Sigsgaard, C., Åkerman, H.J., Foged, N., Blikra, L.H., Pernosky, M.A. and Ødegård, R.S. (2010). 'The thermal state of permafrost in the nordic area during the international polar year 2007–2009', *Permafrost Periglac. Process.*, 21, pp. 156–181.

Christiansen, H. H., Gilbert, G. L., Demidov, N., Gugliemin, M., Isaksen, K., Osuch, M. and Boike, J. (2019) 'Permafrost thermal snapshot and active- layer thickness in Svalbard 2016-2017', In: SESS report 2018 [Orr, E., Hansen, G., Lappalainen, H., Hübner, C. and Lihavainen, H. (eds.)]. *Svalbard Integrated Arctic Earth Observing System*. Available at: https://sios-svalbard.org/sites/sios-svalbard.org/files/common/SESSreport_2018_FullReport.pdf (Accessed: 22 April 2019).

Ebenhoch, S. (2018). *Discussion of the thermo-insulation effect of a seasonal snow cover on permafrost soil in Bayelva, Svalbard (1998 - 2017) with respect to current knowledge.* M.A. Thesis. University of Heidelberg, Germany.

French, H.M. (2007). *The Periglacial Environment.* Chichester, UK: John Wiley & Sons.

Førland, E. J. and Hanssen- Bauer, I. (2000). 'Increased Precipitation in the Norwegian Actic: True or False?', *Climate Change*, 46, pp. 485-509, doi: 10.1023/A:1005613304674.

Førland, E. J., Benestad, R., Hannsen-Bauer, I., Haugen, J. E. and Skaugen, T. E. (2011). 'Temperature and Precipitation Development at Svalbard 1900-2100', *Advances in Meteorology,* vol. 2011, doi:10.1155/2011/893790.

Hanssen- Bauer, I. and Førland, E. J. (1998). ‘Long-term trends in precipitation and temperature in the Norwegian Arctic: can they be explained by changes in atmospheric circulation patterns?’, Climate Research, 10, pp. 143-153.

Bilt, W., Bakke, J.B., Smedsrud, L.H., Sund, M., Schuler, T.V., Westermann, S., Wong, W.K., Sandven, S., Simpson, M., Skogen, M.D., Pavlova, O., Ravndal, O., Risebrobakken, B., Saloranta, T., Mezghani, A., Nilsen, F., Nilsen, J., Nilsen, I.B., Kierulf, H., Kohler, J., Li, H., Lutz, J., Melvold, K., Gjelten, H.M., Gundersen, J., Isaksen, K., Jaedicke, C., Dobler, A., Engeset, R., Frauenfelder, K.R., Gerland, S., Christiansen, H.H., Børsheim, K.Y., Breivik, Ø., Breili, K., Borstad, C.P., Bogen, J., Benestad, R., Beldring, S., Andresen, J., Adakudlu, M., Førland, E., Hisdal, H., Mayer, S., Hanssen-Bauer, I., Sandø and A.B., Sorteberg, A. (2019). Climate in Svalbard 2100 – a knowledge base for climate adaption. Available at: *https://www.miljodirektoratet.no/globalassets/publikasjoner/M1242/M1242.pdf* *(Accessed: 29 April 2019)*

Harris, S. A., French, H. M., Heginbottom, J. A., Johnston, G. H., Ladanyi, B., Sego, D. C., van Everdingen, R. O. (1988). ‘Glossary of Permafrost and Related Ground-Ice Terms’, *National Research Council Canada,* Technical Memorandum, pp. 142.

Hodson, A., Tranter, M., Gurnell, A., Clark, M. and Hagen, J.O. (2002). ‘The hydrochemistry of Bayelva, a high Arctic proglacial stream in Svalbard’, *Journal of Hydrology,* 257 (1-4), pp. 91–114, doi:10.1016/S0022-1694(01)00543-1.

Humlum, O., Instanes, A. and Sollid, J.L. (2003). ‘Permafrost in Svalbard: a review of research history, climatic background and engineering challenges’, *Polar Res.*, 22, pp. 191–215.

Humlum, O. (2005). ’Holocene permafrost aggradation in Svalbard’*, The Geological Society of London, Special Puplications* (Eds C. Harris and J.B. Murton), 242, pp. 119-129.

Isaksen, K., Sollid, J. L., Holmlund, P. and Harris, C. (2007). ‘Recent warming of mountain permafrost in Svalbard and Scandinavia’*, J. Geophys. Res.*, 112, F02S04, doi:10.1029/2006JF000522.

Kokelj, S. V. and Jorgenson, M. T. (2013). ‘Advances in Thermokarst Research’, *Permafrost and Periglacial Processes*, *24*(2), pp. 108–119, doi: 10.1002/ppp.1779.

Lenton, T. M., Held, H., Kriegler, E., Hall, J. W., Lucht, W., Rahmstorf, S. and Schellnhuber, H. J. (2008). ‘Tipping elements in the Earth’s climate system’, *Proceedings of the National Academy of Sciences*, *105*(6), pp. 1786–1793, doi: 10.1073/pnas.0705414105.

Liestøl, O. (1977) ‘Pingos, springs, and permafrost in Spitsbergen’, *Norsk Polarinstitutt, Årbok,* pp. 7-29.

Maturilli, M., Herber, A. and König-Langlo, G. (2015). ‘Surface radiation climatology for Ny-Ålesund, Svalbard (78.9° N), basic observations for trend detection.‘, *Theoretical and Applied Climatology*, 120, pp. 331-339, doi: 10.1007/s00704-014-1173-4.

Nicolsky, D. J. and Romanovsky, V. E. (2018). ‘Modeling Long-Term Permafrost Degradation’, *Journal of Geophysical Research: Earth Surface*, 123(8), pp. 1756-1771, doi: 10.1029/2018JF004655.

Ohtsuka, T., Adachi, M., Uchida, M. and Nakatsubo, T. (2006). 'Relationships between vegetation types and soil properties along a topographical gradient on the northern coast of the Brøgger Peninsula, Svalbard', *Polar Biosci.*, 19, pp. 63-72.

Romanovsky, V. E., Smith, S.L. and Christiansen, H.H. (2010). 'Permafrost thermal state in the polar Northern Hemisphere during the international polar year 2007-2009: a synthesis', *Permafrost Periglacial Processes,* 21 (2), pp. 106–116, doi: 10.1002/ppp.689.

Romanovsky, V. E., Smith, S. L., Christiansen, H. H., Shiklomanov, N. I., Drozdov, D. S., Oberman, N. G., Kholodov, A. L. and Marchenko, S. S. (2011). 'Permafrost', In: Arctic Report Card 2011. Available at: http://www.arctic.noaa.gov/reportcard (Accessed 02 May 2019).

Roth, K. and Boike, J. (2001). 'Quantifying the thermal dynamics of a permafrost site near Ny-Ålesund, Svalbard', *Water Resour. Res.,* 37 (12), pp. 2901–2914, doi: 10.1029/2000WR000163.

Schuur, E. A. G., McGuire, A. D., Schädel, C., Grosse, G., Harden, J. W. Hayes, D.J., Hugelius, G., Koven, C. D., Kuhry, P., Lawrence, D. M., Natali, S. M., Olefeldt, D., Romanovsky, V. E., Schäfer, K., Turetsky, M. R., Treat, C. C. and Vonk, J. E. (2015). 'Climate change and the permafrost carbon feedback', *Nature*, 520, pp. 171-179.

Strand, S.M. (2016). *Ground temperature response to winter warm events in Svalbard*. M.A. Thesis. University of Oslo, Norway. Available at: https://www.duo.uio.no/handle/10852/52107 (Accessed: 1 February 2019)

Vaughan, D.G., Comiso, J.C., Allison, I., Carrasco, J., Kaser, G., Kwok, R., Mote, P., Murray, T., Paul, F., Ren, J., Rignot, E., Solomina, O., Steffen, K. and Zhang, T. (2013). 'Observations: Cryosphere', In: Climate Change 2013: The Physical Science Basis. Contribution of Working Group I to the Fifth Assessment Report of the Intergovernmental Panel on Climate Change [Stocker, T.F., Qin, D., Plattner, G.-K., Tignor, M., Allen, S.K., Boschung, J., Nauels, A., Xia, Y., Bex, V. and Midgley, P.M. (eds.)]. Available at: https://www.ipcc.ch/site/assets/uploads/2018/02/WG1AR5_Chapter04_FINAL.pdf (Accessed: 16 March 2019).

Westermann, S., Boike, J., Langer, M., Schuler, T., and Etzelmüller, B. (2011). 'Modeling the impact of wintertime rain events on the thermal regime of permafrost', *The Cryosphere,* 5, pp. 1697-1736.

Zhang, T., T. Osterkamp, and K. Stamnes (1997). 'Effects of climate on the active layer and permafrost on the north slope of Alaska, USA', *Permafrost Periglacial Processes*, 8(1), pp. 45–67.

Appendix A

Data Description

a) Quality flag system used for all data from Bayelva (Boike et al., 2017a; Boike et al., 2017b)

flag	meaning	description
0	Good data	All quality tests passed
1	No data	Missing value
2	System error	System failure led to corrupted data, e.g. when the power supply broke down, sensors were removed from their proper location, sensors broke or the data logger saved error codes
3	Maintenance	Values influenced by the installation, calibration and cleaning of sensors or programming of the data logger; information from field protocols of engineers
4	Physical limits	Values outside the physically possible or likely limits, e.g. relative humidity should be in a range of 0-100%
5	Gradient	Values unlikely because of prolonged constant periods or high/low spikes; test within each single series
6	Plausibility	Values unlikely in comparison with other series or for a given time of the year; flagged manually by engineers
7	Decreased accuracy	Values with decreased sensor accuracy, e.g. identified when thawing soil does not have a temperature of 0°C
8	Snow covered	Good data, but the sensor is snow covered

b) Names of the parameters at each soil station. Left column: Parameter names for sensors of station (a) in Figure 3 (1998-2012), the ending shows the _x and then the _y (here: depth) coordinate of the sensor; middle: Parameter names for sensors of station (c) in Figure 3 (2009-current) with _x ending showing the depth; right: parameter names of combined dataset which are used in this work with mean depth of the combined sensors (Boike et al., 2017b, Boike et al., 2018).

1998-2012	2009-current	LV2
Ts_a_145_6	Ts_c_1	Ts_lv2_4
Ts_a_169_9	Ts_c_11	Ts_lv2_10
Ts_a_124_25	Ts_c_21	Ts_lv2_23
Ts_a_145_40	Ts_c_37	Ts_lv2_39
Ts_a_145_62	Ts_c_55	Ts_lv2_59
Ts_a_151_76	Ts_c_71	Ts_lv2_74
Ts_a_145_99	Ts_c_89	Ts_lv2_94
Ts_a_135_125_v	Ts_c_141	Ts_lv2_133
Vwc_140_6	Vwc_c_1	Vwc_lv2_4
Vwc_174_8	Vwc_c_11	Vwc_lv2_10
Vwc_115_22	Vwc_c_21	Vwc_lv2_22
Vwc_140_39	Vwc_c_37	Vwc_lv2_38
Vwc_140_62	Vwc_c_55	Vwc_lv2_59
Vwc_146_76	Vwc_c_71	Vwc_lv2_74
Vwc_95_99	Vwc_c_89	Vwc_lv2_94

Appendix B

Monthly liquid precipitation sum in mm for all years and months

NA indicates months with less than 90 % of the daily average data available.

	1998	1999	2000	2001	2002	2003	2004	2005	2006	2007	2008
Jan	NA	NA	0	0.70	NA	0	0.20	4.10	86	0.10	33.20
Feb	NA	NA	0	4	NA	6.90	0	46.10	2.70	0	NA
Mar	NA	NA	0	0	NA	0	1	0	0	0.10	NA
Apr	NA	NA	4.20	4.20	NA	12.90	9.70	0.90	11.20	0.10	NA
May	NA	NA	15.60	NA	NA	19	4.80	0.40	9.50	15.90	4.80
Jun	NA	NA	1.50	NA	10.20	10.20	9.80	2.50	18.40	23.10	9.60
Jul	NA	NA	41.80	NA	13.40	46.20	74.20	58.40	23.20	35.80	36.10
Aug	NA	33.30	20.50	45.70	111.30	26	30.70	33.20	25.70	25.80	14.50
Sep	NA	62.90	118.70	84.50	28.50	31.50	8.50	11	14.50	22.10	96
Oct	NA	11.40	120.80	32.90	114.70	17.10	0.20	12.90	10.80	36.40	6.80
Nov	NA	17	42.50	0	25.10	24	0	3.50	19.40	NA	0
Dec	NA	0.30	0	NA	77.20	0	0	29.40	2.10	3.50	8.30

	2009	2010	2011	2012	2013	2014	2015	2016	2017	2018
Jan	13.80	90.40	0.90	31.40	8.60	18.90	56.30	51.30	5.50	75.70
Feb	12	0	19.20	NA	0.10	7	NA	0	70.30	49.90
Mar	0	0	38.20	NA	0	0	31.80	30.30	0	0
Apr	0	0.40	8.50	NA	3.10	0	16	2.90	8.30	4.20
May	13.20	19.30	16.10	20.30	15.90	22.40	17	23.60	4.70	44
Jun	9.70	5.80	1.60	21.80	63.20	6.60	10.50	12.90	14.20	13.90
Jul	23.60	9	23.30	17.90	60	32.30	11.60	29	25.10	102.30
Aug	23.20	8.80	30.20	29.10	110.20	18	39.60	NA	17.60	58.90
Sep	NA	20.20	63.20	NA	58.90	88.50	94.70	NA	157.60	56.30
Oct	NA	48.90	30.90	26.80	5	32.70	36.50	117.70	45.70	31.20
Nov	77.80	0	52.30	0	0	38.30	13.10	103.90	0	NA
Dec	19.10	1	0	0	5.40	2.30	67	14.10	0	NA

Appendix C

Mean annual soil temperatures and mean annual LVWC

Displayed are all trends and results for the mean annual soil temperature (Ts) and the mean annual LVWC at different depths. Red numbers imply that the trend was significant at $\alpha = 0.05$

Depth	Increase in °C/ decade	Uncertainty in °C/ decade
Ts 4cm	1.1	0.5
Ts 10cm	0.9	0.6
Ts 23cm	1.3	0.5
Ts 39cm	0.9	0.6
Ts 59cm	1.3	0.5
Ts 74cm	1.1	0.6
Ts 94cm	1.5	0.4
Ts 133cm	1.6	0.4

Depth	Increase in %/ decade	Uncertainty in %/ decade
Lvwc 4cm	-1.7	0.6
Lvwc 10cm	2.1	0.8
Lvwc 22cm	2.3	0.8
Lvwc 38cm	0.6	0.9
Lvwc 59cm	2.8	0.9
Lvwc 74cm	3.2	1.2
Lvwc 94cm	3.1	0.8

Appendix D

October Results

All trends and results for the soil temprature (Ts) and the liquid volumetric water content (Vwc) from different depths for the month October. Using the following variable names:

Ts_lv2_4 -> Soil temperature_level 2 data_data from 4cm depth

Vwc_lv2_4 -> Liquid volumetric water content_level2data_from 4cm depth

Prec -> Precipitation in mm

Dsn -> Snow depth in m

T -> Air temperature in 2m in °C

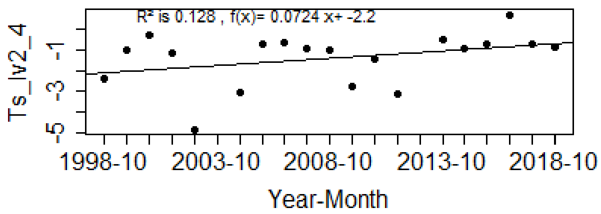

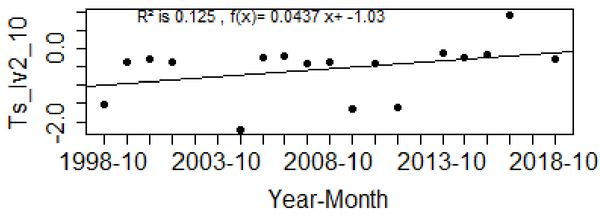

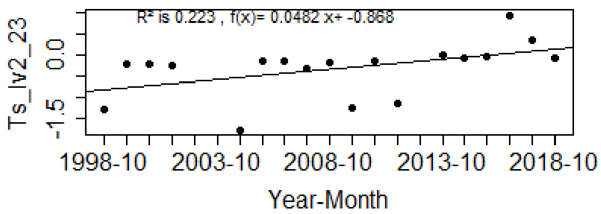

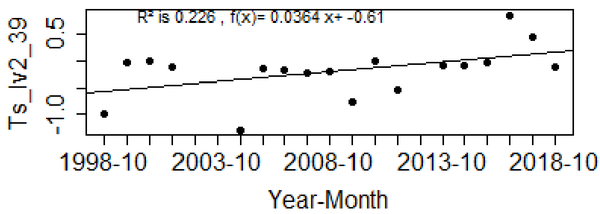

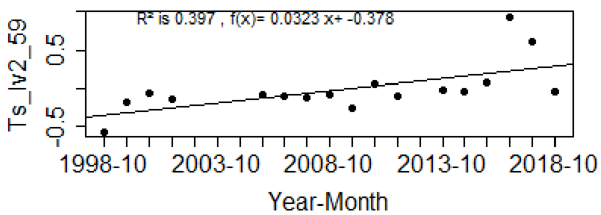

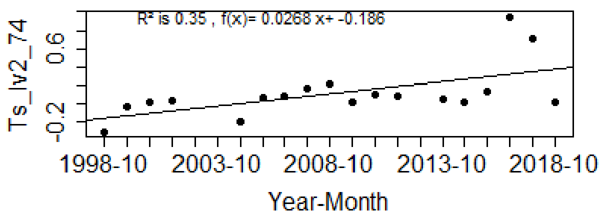

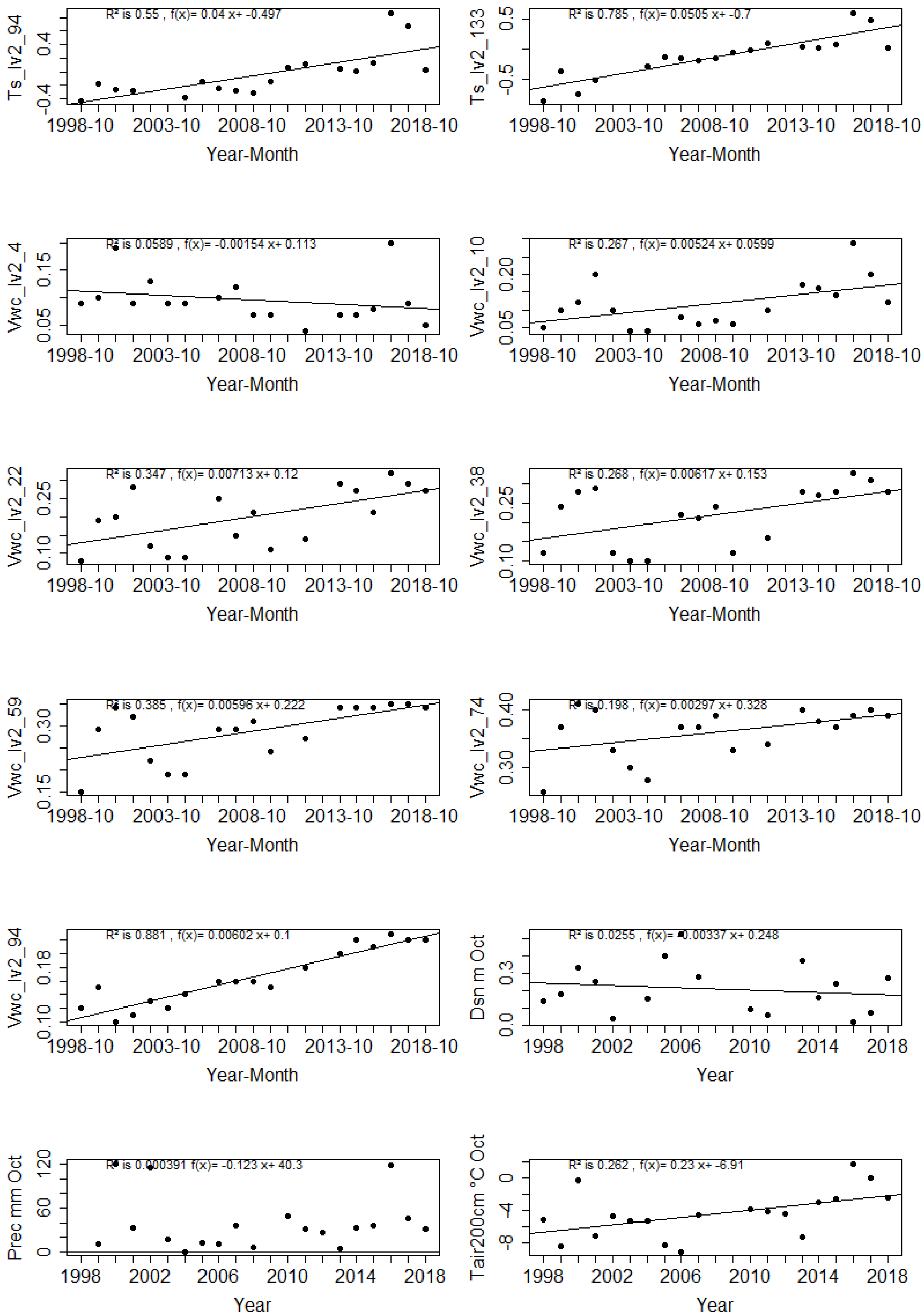
R² is 0.55 , f(x)= 0.04 x+ -0.497
Ts_lv2_94
Year-Month
R² is 0.785 , f(x)= 0.0505 x+ -0.7
Ts_lv2_133
Year-Month
R² is 0.0589 , f(x)= -0.00154 x+ 0.113
Vwc_lv2_4
Year-Month
R² is 0.267 , f(x)= 0.00524 x+ 0.0599
Vwc_lv2_10
Year-Month
R² is 0.347 , f(x)= 0.00713 x+ 0.12
Vwc_lv2_22
Year-Month
R² is 0.268 , f(x)= 0.00617 x+ 0.153
Vwc_lv2_38
Year-Month
R² is 0.385 , f(x)= 0.00596 x+ 0.222
Vwc_lv2_59
Year-Month
R² is 0.198 , f(x)= 0.00297 x+ 0.328
Vwc_lv2_74
Year-Month
R² is 0.881 , f(x)= 0.00602 x+ 0.1
Vwc_lv2_94
Year-Month
R² is 0.0255 , f(x)= -0.00337 x+ 0.248
Dsn m Oct
Year
R² is 0.000391 f(x)= -0.123 x+ 40.3
Prec mm Oct
Year
R² is 0.262 , f(x)= 0.23 x+ -6.91
Tair200cm °C Oct
Year

Appendix E

Increase in soil temperature (Ts) and liquid volumetric water content (Lvwc) in all months and for all depths using the following variable names:

Ts_lv2_4 -> Soil temperature_level 2 data_data from 4cm depth in °C

Lvwc_lv2_4 -> Soil liquid volumetric water content _level 2 data_data from 4cm depth in %

Red marked are trends which are significant at the level α=0.05.

	Jan °C/ decade	Feb °C/ decade	Mar °C/ decade	Apr °C/ decade	May °C/ decade	Jun °C/ decade
Ts_lv2_4	1.0	1.9	1.5	1.3	1.1	1.1
Ts_lv2_10	1.0	2.0	1.5	1.2	1.1	0.8
Ts_lv2_23	1.1	1.7	1.4	1.4	1.2	0.5
Ts_lv2_39	1.1	1.7	1.5	1.3	1.1	0.4
Ts_lv2_59	1.5	1.7	1.6	1.6	1.6	0.6
Ts_lv2_74	1.3	1.5	1.6	1.3	1.3	0.6
Ts_lv2_94	1.6	1.9	1.6	1.9	2.3	1.2
Ts_lv2_133	1.6	1.9	1.7	1.5	1.7	1.0

	Jul °C/ decade	Aug °C/ decade	Sep °C/ decade	Oct °C/ decade	Nov °C/ decade	Dec °C/ decade
Ts_lv2_4	0.5	0.5	0.8	0.7	-0.6	-0.2
Ts_lv2_10	0.7	0.6	0.5	0.4	-0.2	0.4
Ts_lv2_23	0.6	0.7	0.6	0.5	-0.5	-0.5
Ts_lv2_39	0.6	0.8	0.4	0.4	0.2	0.4
Ts_lv2_59	0.9	1.1	0.6	0.3	0.2	-0.4
Ts_lv2_74	0.7	1.2	0.6	0.3	0.3	-0.2
Ts_lv2_94	1.2	1.7	1.0	0.4	0.2	-0.2
Ts_lv2_133	0.8	1.3	0.9	0.5	0.6	0.7

	Jan %/ decade	Feb %/ decade	Mar %/ decade	Apr %/ decade	May %/ decade	Jun %/ decade
Lvwc_lv2_4	-1.2	-0.2	-0.3	-0. 4	-0. 9	-0. 6
Lvwc_lv2_10	1.5	1.9	1.3	1.3	1.4	4.7
Lvwc_lv2_22	1.6	1.7	1.6	1.4	0. 9	4.6
Lvwc_lv2_38	-0.4	-0.2	-0.3	-0. 4	-0. 9	0. 8
Lvwc_lv2_59	2.5	2.3	1.8	1.6	1.4	2.3
Lvwc_lv2_74	5.1	3.0	2.8	2.5	2.5	2.4
Lvwc_lv2_94	1.7	1.0	1.0	1.1	0. 7	0. 8

	Jul %/ decade	Aug %/ decade	Sep %/ decade	Oct %/ decade	Nov %/ decade	Dec %/ decade
Lvwc_lv2_4	-4.7	-4.5	-1.3	-1.5	-2.6	-2.3
Lvwc_lv2_10	-1.0	-1.8	2.7	5.2	2.3	1.7

Lvwc_lv2_22	0. 4	-0. 4	2.2	7.1	2.8	1.1
Lvwc_lv2_38	0. 7	-1.1	1.4	6.2	2.2	-1.7
Lvwc_lv2_59	3.6	0. 7	1.4	6.0	5.1	2.9
Lvwc_lv2_74	3.5	-0. 6	-0. 5	3.0	5.8	5.4
Lvwc_lv2_94	5.4	5.0	4.2	6.0	6.1	3.0

Appendix F

Correlation matrices for studied months

Ts_lv2_4 -> Mean soil temperature_level 2 data_data from 4cm depth in °C

Vwc_lv2_4 -> Mean liquid volumetric water content_level2data_from 4cm depth in decimal numbers

snow -> Mean snow depth of current month in m

P -> Liquid precipitation sum of current month in mm; P-1 -> Liquid precipitation sum of previous month in mm

T ->Mean air temperature of this month in 2m in °C; T-1-> mean air temeprature of previous month in °C

October:

	Vwc_lv2_4	Vwc_lv2_10	Vwc_lv2_22	Vwc_lv2_38	Vwc_lv2_59	Vwc_lv2_74	Vwc_lv2_94	Ts_lv2_4	Ts_lv2_10	Ts_lv2_23	Ts_lv2_39	Ts_lv2_59	Ts_lv2_74	Ts_lv2_94	Ts_lv2_133	snow	T	P	Days_Soil_Frozen	Start_Freeze_in	End_Freeze_in
Vwc_lv2_4	1	0.36	0.13	0.24	0.14	0.19	-0.2	0.3	0.48	0.42	0.47	0.47	0.44	0.26	-0.05	-0.09	0.45	0.79	-0.04	0.29	0.13
Vwc_lv2_10		1	0.84	0.81	0.73	0.65	0.56	0.57	0.74	0.78	0.83	0.83	0.75	0.81	0.58	-0.26	0.51	0.45	-0.38	0.77	0.37
Vwc_lv2_22			1	0.94	0.9	0.86	0.63	0.78	0.87	0.89	0.86	0.7	0.63	0.61	0.54	0.22	0.27	0.11	-0.61	0.56	0.64
Vwc_lv2_38				1	0.95	0.9	0.56	0.87	0.94	0.95	0.93	0.72	0.63	0.59	0.43	0.2	0.41	0.21	-0.55	0.58	0.59
Vwc_lv2_59					1	0.96	0.61	0.77	0.84	0.87	0.87	0.67	0.6	0.57	0.53	0.23	0.39	0.2	-0.63	0.54	0.66
Vwc_lv2_74						1	0.42	0.72	0.82	0.83	0.83	0.56	0.53	0.41	0.37	0.32	0.27	0.23	-0.54	0.4	0.62
Vwc_lv2_94							1	0.43	0.45	0.56	0.54	0.64	0.59	0.77	0.89	-0.18	0.43	-0.07	-0.65	0.61	0.55
Ts_lv2_4								1	0.97	0.94	0.87	0.64	0.6	0.46	0.31	0.41	0.23	-0.04	-0.61	0.48	0.69
Ts_lv2_10									1	0.99	0.96	0.77	0.7	0.56	0.41	0.21	0.27	0.47	-0.59	0.49	0.68
Ts_lv2_23										1	0.97	0.82	0.74	0.65	0.53	0.06	0.37	0.48	-0.5	0.57	0.56
Ts_lv2_39											1	0.91	0.81	0.74	0.58	-0.08	0.46	0.6	-0.41	0.68	0.45
Ts_lv2_59												1	0.97	0.92	0.8	-0.4	0.65	0.58	-0.31	0.88	0.3
Ts_lv2_74													1	0.88	0.79	-0.35	0.61	0.54	-0.36	0.88	0.35
Ts_lv2_94														1	0.86	-0.51	0.66	0.49	-0.27	0.89	0.2
Ts_lv2_133															1	-0.34	0.43	0.12	-0.49	0.75	0.4
snow																1	-0.54	-0.42	-0.52	-0.39	0.6
T																	1	0.68	0.06	0.61	-0.08
P																		1	0.14	0.32	-0.12
Days_Soil_Frozen																			1	-0.27	-0.97
Start_Freeze_in																				1	0.24
End_Freeze_in																					1

<u>February:</u>

	Vwc_lv2_4	Vwc_lv2_10	Vwc_lv2_22	Vwc_lv2_38	Vwc_lv2_59	Vwc_lv2_74	Vwc_lv2_94	Ts_lv2_4	Ts_lv2_10	Ts_lv2_23	Ts_lv2_39	Ts_lv2_59	Ts_lv2_74	Ts_lv2_94	Ts_lv2_133	snow	T	P	PWin	Freeze Start	Freeze End	Days_Soil_Frozen	Max_Snow_Depth
Vwc_lv2_4	1	0.54	0.73	0.78	0.68	0.61	0.59	0.54	0.49	0.56	0.59	0.58	0.58	0.5	0.46	0.54	0.11	-0.15	0.14	0.06	0.37	-0.63	-0.27
Vwc_lv2_10		1	0.8	0.47	0.63	0.63	0.37	0.51	0.55	0.5	0.61	0.61	0.58	0.58	0.61	0.36	0.42	0.25	0.31	0.37	0.37	-0.65	-0.3
Vwc_lv2_22			1	0.85	0.94	0.9	0.76	0.85	0.88	0.87	0.89	0.89	0.88	0.89	0.88	0.51	0.32	0.1	0.24	0.1	0.39	-0.88	-0.18
Vwc_lv2_38				1	0.89	0.87	0.82	0.72	0.76	0.75	0.77	0.77	0.77	0.76	0.68	0.59	0.18	-0.17	-0.03	-0.18	0.29	-0.79	-0.01
Vwc_lv2_59					1	0.95	0.86	0.91	0.91	0.93	0.92	0.92	0.92	0.91	0.88	0.61	0.31	0.02	0.21	[illegible]	0.35	-0.89	-0.11
Vwc_lv2_74						1	0.89	0.91	0.88	0.94	0.91	0.92	0.92	0.97	0.95	0.58	0.25	[illegible]	0.22	0.17	0.33	-0.93	-0.05
Vwc_lv2_94							1	0.73	0.79	0.76	0.83	0.84	0.85	0.83	0.79	0.48	0.27	0.03	0.28	0.11	0.47	-0.81	0.13
Ts_lv2_4								1	1	0.99	0.99	0.98	0.97	0.96	0.92	0.75	0.44	0.15	0.68	0.08	0.07	-0.75	-0.07
Ts_lv2_10									1	1	0.99	0.99	0.98	0.96	0.92	0.57	0.55	0.27	0.73	0.2	0.24	-0.7	-0.03
Ts_lv2_23										1	1	0.99	0.99	0.97	0.92	0.74	0.43	0.21	0.76	0.15	0.1	-0.72	-0.12
Ts_lv2_39											1	1	1	0.98	0.95	0.59	0.43	0.17	0.41	0.17	0.31	-0.79	-0.14
Ts_lv2_59												1	1	0.99	0.96	0.57	0.4	0.16	0.42	0.18	0.31	-0.81	-0.15
Ts_lv2_74													1	0.99	0.96	0.57	0.38	0.15	0.44	0.18	0.3	-0.81	-0.14
Ts_lv2_94														1	0.99	0.49	0.47	0.25	0.76	0.33	0.28	-0.85	-0.07
Ts_lv2_133															1	0.44	0.44	0.26	0.75	0.41	0.34	-0.87	-0.11
snow																1	0.03	-0.19	0.37	-0.1	0.1	-0.43	-0.12
T																	1	0.45	0.09	0.16	0.33	-0.33	0.22
P																		1	0.47	0.16	-0.06	-0.07	-0.4
PWin																			1	0.43	0.12	-0.25	-0.12
Freeze Start																				1	0.24	-0.36	-0.14
Freeze End																					1	-0.34	0.37
Days_Soil_Frozen																						1	0.07
Max_Snow_Depth																							1

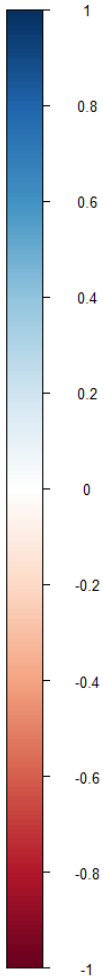

April:

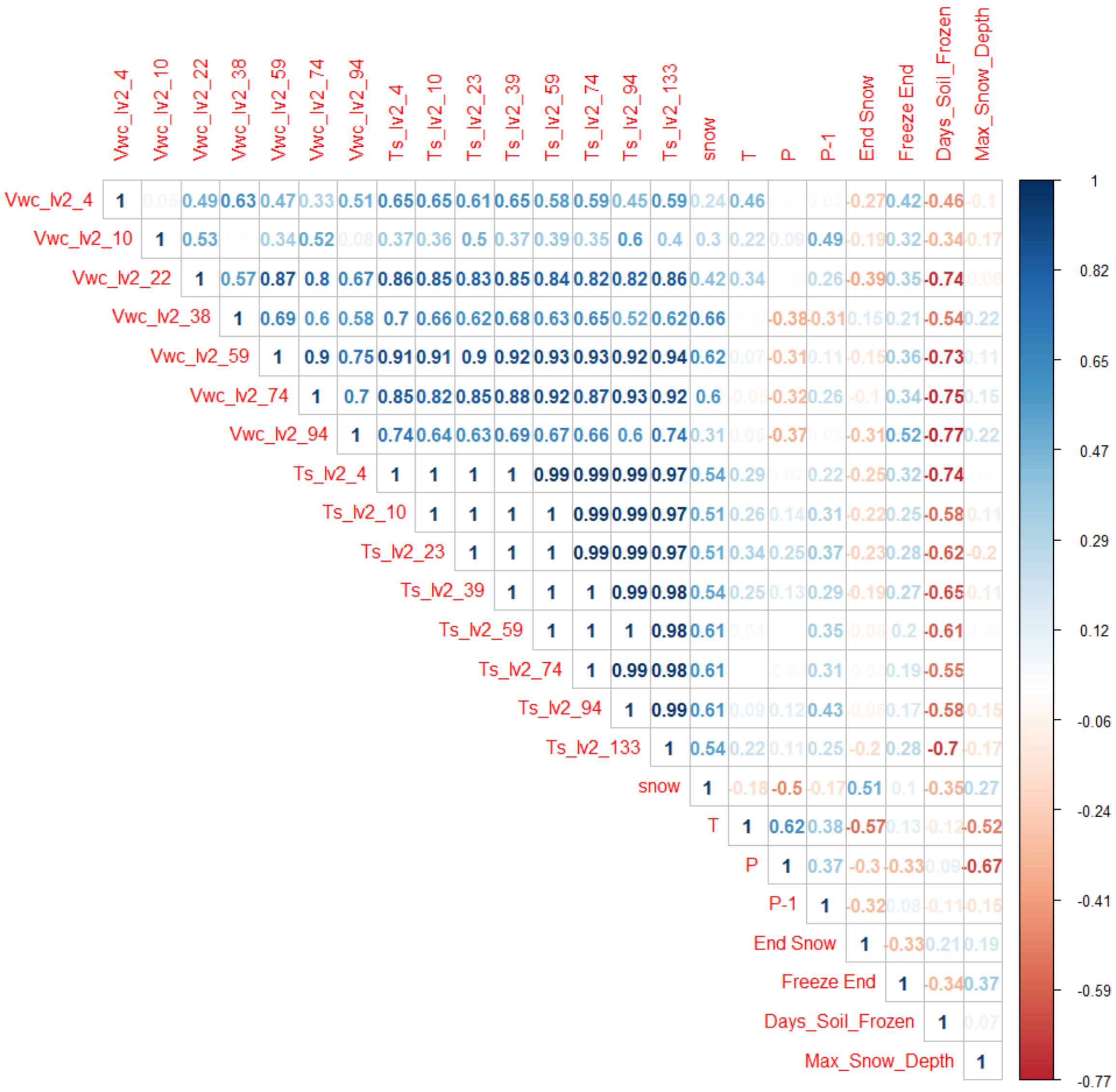
Vwc_lv2_4
Vwc_lv2_10
Vwc_lv2_22
Vwc_lv2_38
Vwc_lv2_59
Vwc_lv2_74
Vwc_lv2_94
Ts_lv2_4
Ts_lv2_10
Ts_lv2_23
Ts_lv2_39
Ts_lv2_59
Ts_lv2_74
Ts_lv2_94
Ts_lv2_133
snow
T
P
P-1
End Snow
Freeze End
Days_Soil_Frozen
Max_Snow_Depth
1
0.82
0.65
0.47
0.29
0.12
-0.06
-0.24
-0.41
-0.59
-0.77

July:

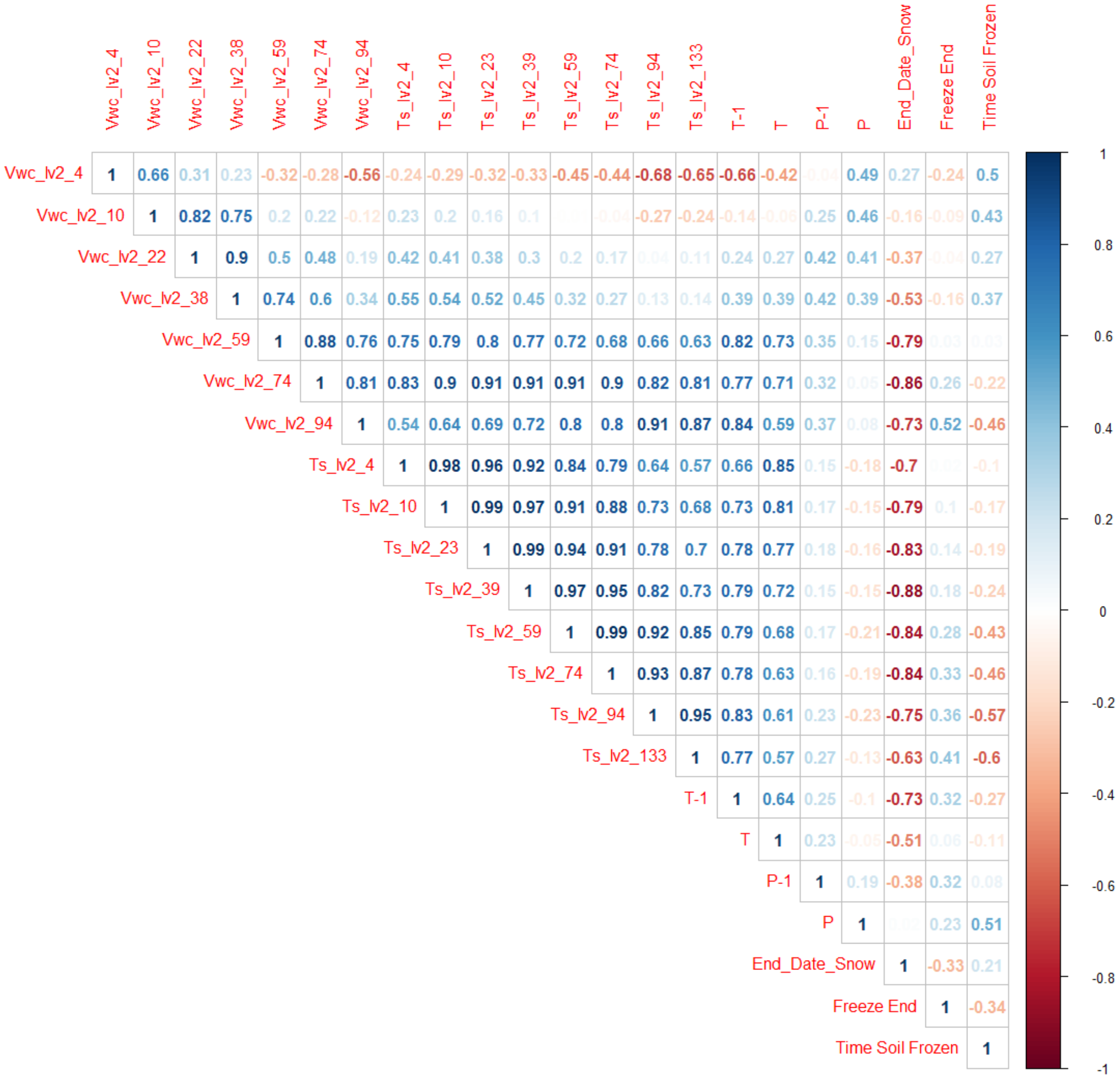
Vwc_lv2_4
Vwc_lv2_10
Vwc_lv2_22
Vwc_lv2_38
Vwc_lv2_59
Vwc_lv2_74
Vwc_lv2_94
Ts_lv2_4
Ts_lv2_10
Ts_lv2_23
Ts_lv2_39
Ts_lv2_59
Ts_lv2_74
Ts_lv2_94
Ts_lv2_133
T-1
T
P-1
P
End_Date_Snow
Freeze End
Time Soil Frozen
Vwc_lv2_4 1 0.66 0.31 0.23 -0.32 -0.28 -0.56 -0.24 -0.29 -0.32 -0.33 -0.45 -0.44 -0.68 -0.65 -0.66 -0.42 0.04 0.49 0.27 -0.24 0.5
Vwc_lv2_10 1 0.82 0.75 0.2 0.22 -0.12 0.23 0.2 0.16 0.1 -0.04 -0.27 -0.24 -0.14 -0.06 0.25 0.46 -0.16 -0.09 0.43
Vwc_lv2_22 1 0.9 0.5 0.48 0.19 0.42 0.41 0.38 0.3 0.2 0.17 0.04 0.11 0.24 0.27 0.42 0.41 -0.37 0.04 0.27
Vwc_lv2_38 1 0.74 0.6 0.34 0.55 0.54 0.52 0.45 0.32 0.27 0.13 0.14 0.39 0.39 0.42 0.39 -0.53 -0.16 0.37
Vwc_lv2_59 1 0.88 0.76 0.75 0.79 0.8 0.77 0.72 0.68 0.66 0.63 0.82 0.73 0.35 0.15 -0.79 0.03 0.03
Vwc_lv2_74 1 0.81 0.83 0.9 0.91 0.91 0.91 0.9 0.82 0.81 0.77 0.71 0.32 0.05 -0.86 0.26 -0.22
Vwc_lv2_94 1 0.54 0.64 0.69 0.72 0.8 0.8 0.91 0.87 0.84 0.59 0.37 0.08 -0.73 0.52 -0.46
Ts_lv2_4 1 0.98 0.96 0.92 0.84 0.79 0.64 0.57 0.66 0.85 0.15 -0.18 -0.7 0.02 -0.1
Ts_lv2_10 1 0.99 0.97 0.91 0.88 0.73 0.68 0.73 0.81 0.17 -0.15 -0.79 0.1 -0.17
Ts_lv2_23 1 0.99 0.94 0.91 0.78 0.7 0.78 0.77 0.18 -0.16 -0.83 0.14 -0.19
Ts_lv2_39 1 0.97 0.95 0.82 0.73 0.79 0.72 0.15 -0.15 -0.88 0.18 -0.24
Ts_lv2_59 1 0.99 0.92 0.85 0.79 0.68 0.17 -0.21 -0.84 0.28 -0.43
Ts_lv2_74 1 0.93 0.87 0.78 0.63 0.16 -0.19 -0.84 0.33 -0.46
Ts_lv2_94 1 0.95 0.83 0.61 0.23 -0.23 -0.75 0.36 -0.57
Ts_lv2_133 1 0.77 0.57 0.27 -0.13 -0.63 0.41 -0.6
T-1 1 0.64 0.25 -0.1 -0.73 0.32 -0.27
T 1 0.23 -0.05 -0.51 0.06 -0.11
P-1 1 0.19 -0.38 0.32 0.08
P 1 0.02 0.23 0.51
End_Date_Snow 1 -0.33 0.21
Freeze End 1 -0.34
Time Soil Frozen 1
1
0.8
0.6
0.4
0.2
0
-0.2
-0.4
-0.6
-0.8
-1